Received: 9 March 2023 | Revised: 19 December 2023 | Accepted: 26 December 2023

DOI: 10.1111/tra.12930

RESEARCH ARTICLE

Traffic WILEY

Glucocorticoids rescue cell surface trafficking of R451C Neuroligin3 and enhance synapse formation

Tamara Diamanti[1] | Laura Trobiani[2] | Lorenza Mautone[3,4] | Federica Serafini[1] | Roberta Gioia[1] | Laura Ferrucci[5] | Clotilde Lauro[5] | Sara Bianchi[1] | Camilla Perfetto[1] | Stefano Guglielmo[1] | Raimondo Sollazzo[1] | Ezio Giorda[6] | Andrea Setini[1] | Davide Ragozzino[5] | Elena Miranda[1] | Davide Comoletti[2,7] | Silvia Di Angelantonio[4,5,8] | Emanuele Cacci[1] | Antonella De Jaco[1]

[1]Department of Biology and Biotechnologies "Charles Darwin", Sapienza University of Rome, Rome, Italy

[2]School of Biological Sciences, Victoria University of Wellington, Wellington, New Zealand

[3]Department of Biochemical Sciences "A. Rossi Fanelli", Sapienza University, Rome, Italy

[4]Center for Life Nano- & Neuro-Science, Fondazione Istituto Italiano di Tecnologia (IIT), Rome, Italy

[5]Department of Physiology and Pharmacology "V. Erspamer", Sapienza University of Rome, Rome, Italy

[6]Ospedale Pediatrico Bambino Gesù, Rome, Italy

[7]Child Health Institute of New Jersey, Rutgers University, New Brunswick, New Jersey, USA

[8]D-tails s.r.l. Via di Torre Rossa, Rome, Italy

Correspondence
Antonella De Jaco and Emanuele Cacci, Department of Biology and Biotechnologies "Charles Darwin", Sapienza University of Rome, P.le Aldo Moro 5, Rome 00185, Italy.
Email: antonella.dejaco@uniroma1.it and emanuele.cacci@uniroma1.it

Funding information
REGIONE LAZIO, Grant/Award Numbers: A0112E0073, 19036AP000000019; Fulbright Award, Grant/Award Number: FSP-P005556; Sapienza University; D-Tails-IIT JointLab;

Abstract

Neuroligins are synaptic cell adhesion proteins with a role in synaptic function, implicated in neurodevelopmental disorders. The autism spectrum disorder-associated substitution Arg451Cys (R451C) in NLGN3 promotes a partial misfolding of the extracellular domain of the protein leading to retention in the endoplasmic reticulum (ER) and the induction of the unfolded protein response (UPR). The reduced trafficking of R451C NLGN3 to the cell surface leads to altered synaptic function and social behavior. A screening in HEK-293 cells overexpressing NLGN3 of 2662 compounds (FDA-approved small molecule drug library), led to the identification of several glucocorticoids such as alclometasone dipropionate, desonide, prednisolone sodium phosphate, and dexamethasone (DEX), with the ability to favor the exit of full-length R451C NLGN3 from the ER. DEX improved the stability of R451C NLGN3 and trafficking to the cell surface, reduced the activation of the UPR, and increased the formation of artificial synapses between HEK-293 and hippocampal primary neurons. The effect of DEX was validated on a novel model system represented by neural stem progenitor cells and differentiated neurons derived from the R451C NLGN3 knock-in mouse, expressing the endogenous protein. This work shows a potential rescue strategy for an autism-linked mutation affecting cell surface trafficking of a synaptic protein.

KEYWORDS
autism spectrum disorders, dexamethasone, ER stress, neural stem progenitor cells, neurodevelopmental disorder, neurons, synaptic contacts, synaptic protein, unfolded protein response

Abbreviations: AD, alclometasone dipropionate; ATF6, activating transcription factor; FDA, American Food and Drugs Administration; R451C, Arg451Cys; ASDs, autism spectrum disorders; CHX, cycloheximide; Delta NS, delta neuroserpin; D, desonide; DEX, dexamethasone; ER, endoplasmic reticulum; GR, glucocorticoid receptor; GCs, glucocorticoids; BiP, immunoglobulin heavy-chain-binding protein; Ire1, inositol-requiring enzyme 1; NSPCs, neural stem progenitor cells; NLGN, neuroligin; PSP, prednisolone sodium phosphate; PDI, protein disulfide isomerase; PERK, protein kinase-like endoplasmic reticulum kinase; UPR, unfolded protein response; WT, wild type.

Robert Wood Johnson Foundation to the Child Health Institute of New Jersey, Grant/Award Number: 74260; Governor's Council for Medical Research and Treatment of Autism, Grant/Award Number: CAUT16APL020

1 | INTRODUCTION

The neuroligin (NLGN) family of postsynaptic cell adhesion molecules plays a major role in regulating synapse formation and maturation during brain development.[1] Mutations associated with autism spectrum disorders (ASDs) in genes encoding for the NLGN proteins have been reported to affect either the synthesis or the folding and trafficking of the mutant proteins.[2–4] There are five members in the NLGN family in humans and other primates: NLGN1, 2, 3, 4X, and 4Y.[5–8] Among the NLGNs, the highest number of ASDs-associated mutations have been found in the *NLGN3* and *NLGN4* genes,[9–11] although ASDs-mutations have been recently mapped in the *NLGN1* and *NLGN2* genes.[12,13] It is noteworthy that most of the mutations result in residue substitutions impairing the folding of the extracellular domain, therefore causing the retention of the mutant protein in the endoplasmic reticulum (ER).[4] Ultimately, this leads to a reduced trafficking of the mutant protein to the cell surface causing functional and behavioral alterations.[14] Among the NLGNs variants, the R451C substitution in NLGN3 was one of the first mutations to be reported in association with ASDs. The cysteine residue replacing the arginine at position 451 causes a local misfolding in the structure of the extracellular domain of the protein, leading to a slowdown in the maturation process of NLGN3.[15,16] Therefore, mutant R451C NLGN3 is retained in the ER through the persistent association with molecular chaperones, it is degraded at a high rate by the proteasome,[15,16] and consequently the amount of mutant protein reaching the cell surface is reduced. At the functional level, the purified mutant protein is unable to associate with neurexin[17] and when exposed on the surface of a heterologous system, it has reduced capacity to form synapses in transfected hippocampal neurons.[18] In the *knock-in* mouse strain expressing the R451C mutation, mutant endogenous NLGN3 is highly unstable and is promptly degraded by the proteasome. Consequently, NLGN3 protein levels in the brain are reduced to around 10% compared with its levels in the parental mice strain.[19,20] Consistent to the in vitro findings, the mutant protein is retained in the ER and degraded by the proteasome also in vivo.[21] The accumulation of misfolded proteins in the ER can lead to a cellular stress condition and to the activation of the unfolded protein response (UPR), a signaling pathway that aims at reducing the stress in the organelle by enhancing protein folding capacity and proteasome-mediated degradation, while attenuating protein synthesis.[22] The ER-retention of R451C NLGN3 activates the UPR, both in vitro and in vivo. Interestingly, in the R451C NLGN3 mouse brain, the activation of UPR is specific to the cerebellum, where the UPR modulates neurotransmission.[21,23] In agreement with this, it has been recently shown that other ASDs mutations cause retention of mutant NLGN3 in the ER and UPR activation.[24] In recent years, several studies have focused on developing treatments for correcting protein misfolding and impaired trafficking, and attenuating the UPR by using disease model systems both in vitro and in vivo. UPR signaling is crucial in several diseases, particularly in those involving highly secretory cell types, like neurons.[25,26] Since the nature of the misfolding caused by the R451C substitution is confined to a superficial loop of the acetylcholinesterase-like domain, we have used this mutant protein to select compounds to restore NLGN3 trafficking to the cell surface.

In this work, using an FDA-approved small molecule drug library (2662 compounds), we have identified several compounds, some of which belonging to the glucocorticoids (GCs) family, that favor NLGN3 trafficking, both for the wild type (WT) and R451C forms. Specifically, we have shown that Dexamethasone (DEX) favors the exit of R451C NLGN3 from the ER and improves its trafficking to the cell surface. Our results showed that GCs mitigate ER stress and enhance the formation of artificial synapses. Isolated neural stem progenitor cells (NSPCs) can be propagated and differentiated in vitro, maintaining high neurogenic potential and representing a valuable tool for studying the mechanisms of several diseases.[27] With the goal of confirming our results in a cell model that express either WT or R451C NLGN3 as endogenous proteins, we have isolated NSPCs from the dentate gyrus of the hippocampus of adult WT and knock-in R451C NLGN3 mouse strains and established a novel model system for studying the molecular mechanisms underlying a monogenic form of ASDs. Cell cultures derived from the R451C NLGN3 mice showed reduced levels of mutant NLGN3 due to proteasomal degradation, as previously observed in other cell-based systems. Interestingly, we found that DEX treatment increased mutant NLGN3 protein levels both in proliferative and differentiated conditions and reduced ER stress, suggesting that the selected compound is also effective in a cell model expressing the endogenous protein of this form of ASDs.

2 | RESULTS

2.1 | GCs improve the trafficking of both soluble and full-length R451C NLGN3

A library of 2662 compounds (FDA-approved small molecule drug library) was screened for molecules that improve the trafficking of R451C NLGN3. We have used a fluorescent approach, based on HEK-293 cells engineered to produce a truncated form of NLGN3, lacking the transmembrane and intracellular domains, and C-terminally fused to the fluorescent protein Venus (NLGN3-Venus).[28] The resulting cell lines produce a fluorescent NLGN3, either WT or R451C, which is secreted by the cells, therefore allowing the quantification of protein trafficking by measuring fluorescence levels in the cell culture medium. In this

TABLE 1 FDA-approved compounds selected after a wide screening for increasing R451C NLGN3 protein levels.

Name	Abbreviations	Chemical class	Molecular formula
Alclometasone dipropionate	AD	Glucocorticoid	$C_{28}H_{37}ClO_7$
Betamethasone acetate	BA	Glucocorticoid	$C_{24}H_{31}FO_6$
Carbenoxolone sodium	CBX	Glycyrrhetinic acid derivate with a steroide-like structure	$C_{34}H_{48}Na_2O_7$
Desonide	D	Glucocorticoid	$C_{24}H_{32}O_6$
Desoxymetasone	DES	Glucocorticoid	$C_{22}H_{29}FO_4$
Dexamethasone	DEX	Glucocorticoid	$C_{22}H_{29}FO_5$
Ethylnorepinephrine hydrochloride	EH	Norepinephrine derivate	$C_{10}\ H_{16}ClNO_3$
Isoflupredone acetate	IA	Glucocorticoid	$C_{23}H_{29}FO_6$
Milnacipran hydrochloride	MH	Phenylacetic acids derivate	$C_{15}H_{23}ClN_2O$
Phenylethyl alcohol	PA	Alcohol	$C_8H_{10}O$
Phenytoin sodium	PS	Imadazole derivate	$C_{15}H_{11}N_2NaO_2$
Prednisolone sodium phosphate	PSP	Glucocorticoid	$C_{21}H_{29}Na_2O_8P$
Quinestrol	Q	Synthetic estrogen	$C_{25}H_{32}O_2$

system, due to the retention of the mutant protein in the ER, the cell line expressing R451C NLGN3-Venus shows around 50% reduction in the amount of the secreted protein in comparison to cells expressing the WT protein, as shown before.[28] Each compound was added to the medium 24 h after seeding, at the concentration of 2 μM, and the fluorescence signal was measured after 60 h, to allow the mutant and fluorescent protein to accumulate in the medium. The initial screening was conducted using only the cell line expressing R451C NLGN3-Venus. After this first screening, 13 compounds (see Table 1) were identified for their ability to increase the fluorescence levels in the culture medium at least two-fold, in comparison to the untreated R451C NLGN3-Venus control condition (Figure 1A). Most of the compounds we identified belonged to the GCs family.

After this first screening, 4 out of the 13 compounds that showed activity were selected for further analysis: alclometasone dipropionate (AD), desonide (D), prednisolone sodium phosphate (PSP) and DEX. These GCs were further tested for their effect on the full-length NLGN3 protein form. HEK-293 cell lines stably expressing NLGN3, either WT or R451C, were generated and the GCs were administered at the concentration of 2 μM for 48 h.

Western blot analysis by using the anti-NLGN3/FLAG antibody (Anti-FLAG, Sigma-Aldrich no. F7425) detected a single band in the lysates expressing the WT form that corresponds to the fully processed form of the protein, while R451C NLGN3 appeared as two distinct bands representing the unprocessed and the mature forms as previously described in De Jaco et al.[29] For the densitometric analysis, the signal resulting from the two bands together, was always considered.

No significant increase in protein levels, in cell lysates, was observed for the WT protein after treatment (Figure 1B). Instead, full-length R451C NLGN3 levels increased significantly after treatment with each of the four GCs, in line with what was previously observed for the secreted form (Figure 1C). Changes in the intracellular localization of R451C NLGN3 after GCs administration were assessed by coimmunostaining with the ER-resident protein calreticulin. HEK-293 cells expressing full-length WT NLGN3, which shows a physiological localization on the cell surface, were used as control. The decrease in colocalization of NLGN3 with calreticulin was used to quantify the activity of each compound (Figure 2A). The correlation coefficient for colocalization in cells expressing WT NLGN3 was half of that shown by untreated cells expressing the mutant protein (Figure 2B), suggesting a significantly higher retention of R451C NLGN3 in the ER, in agreement with our previous results.[29] Interestingly, the treatment with each of the four GCs significantly reduced the correlation coefficient in cells expressing R451C NLGN3, when compared with the untreated condition (Figure 2B), suggesting a positive effect on protein trafficking.

To quantify the fraction of protein reaching the cell membrane resulting from the treatment with GCs, we used a cytofluorimetric analysis conducted on intact cells (Figure 2C). The intensity values relative to the fluorescence present on the cell membrane (FITC-A) are reported in Table 2. The average FITC-A signal in HEK-293 cells expressing either WT or R451C NLGN3 following the treatments was higher compared with the untreated cells for both genotypes. These results suggest an effect of GCs on the cell surface trafficking of NLGN3 and a rescue effect on the R451C protein with respect to the WT untreated condition. Moreover, we investigated the levels of the extracellular cleaved domain of NLGN3, in the culture medium by western blot, and found that treatment with the selected GCs increased the levels of cleaved R451C NLGN3 (Figure 2D,E).

2.2 | Enhanced R451C NLGN3 protein levels are dependent on the activation of the glucocorticoid receptor

The mechanism of action of GCs usually relies on pleiotropic effects of the GC receptor (GR) on several transcriptional pathways. GR activity is modulated by posttranslational modifications, such as phosphorylation at Ser211, which is increased after GCs administration.[30] To

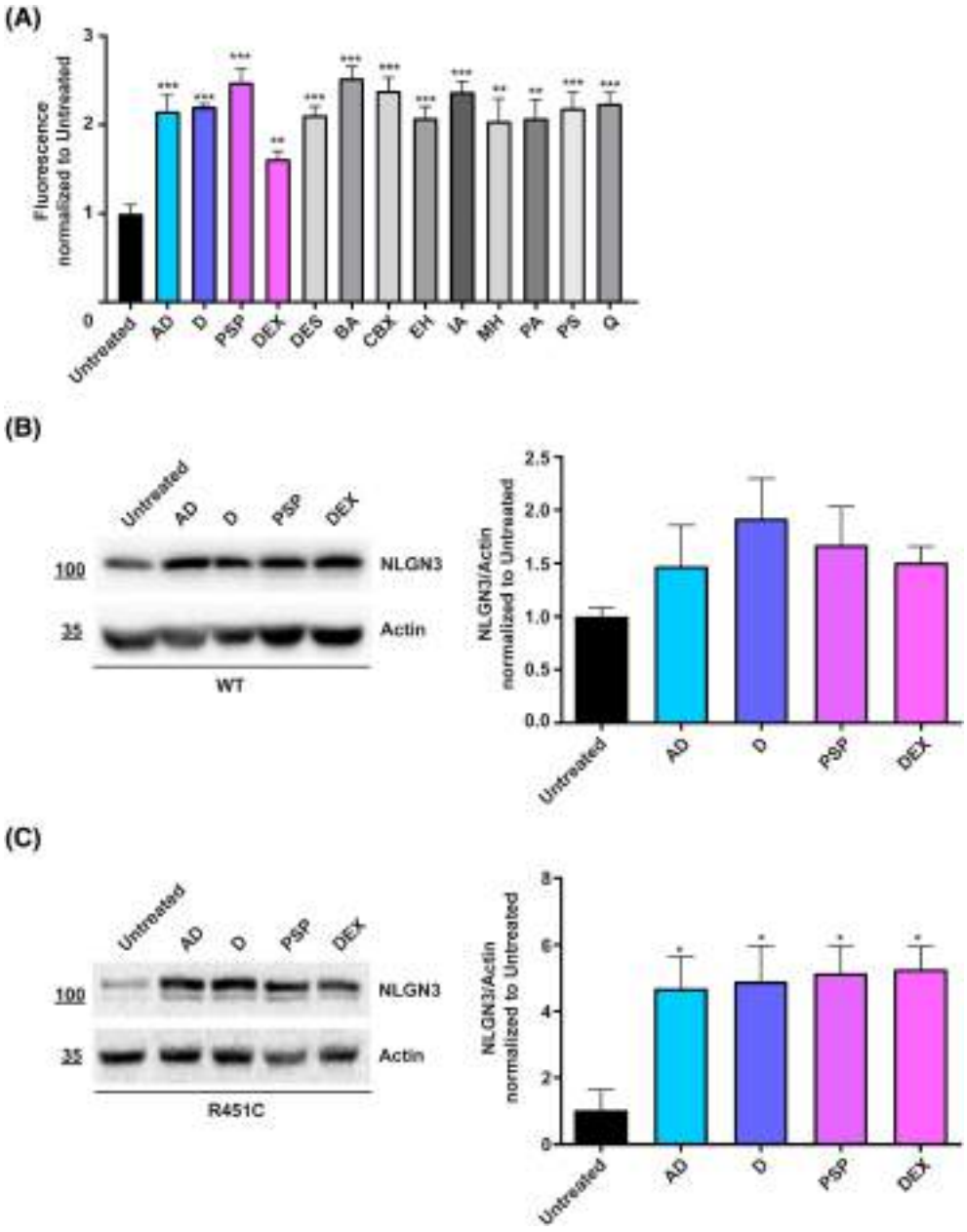

FIGURE 1 Identification of glucocorticoids as enhancers of R451C NLGN3 secretion by screening of an FDA-approved library of compounds. (A) Fluorescence levels in cell culture medium of HEK-293 expressing R451C NLGN3-Venus treated with the indicated compounds at 2 μM for 60 h (see Table 1), normalized to untreated (mean ± SEM; $n = 4$; unpaired t-test). (B,C) Representative western blot and densitometric analysis of NLGN3 levels in lysates of HEK-293 cells expressing wild type (B) or R451C NLGN3 (C) either untreated or treated with the indicated compounds (2 μM for 48 h), normalized to the untreated condition (mean ± SEM; $n = 3$; Unpaired t-test $^{*}p < 0.05$, $^{**}p < 0.01$, $^{***}p < 0.001$). AD, alclometasone dipropionate; D, desonide; DEX, dexamethasone; PSP, prednisolone sodium phosphate.

investigate the involvement of the GR in mediating the effects of GCs on R451C NLGN3 protein levels, we analyzed the phosphorylation of the receptor at Ser211 in lysates of cells expressing either WT or R451C NLGN3, untreated or treated with AD, D, PSP, or DEX. A significant increase in phosphorylation levels was observed in the lysates from both cell lines after treatment with GCs in comparison to untreated conditions (Figure 3A). The combined treatment with the GR antagonist mifepristone (RU486) and DEX significantly reduced the effect of DEX on R451C NLGN3 levels, while having no effect on WT NLGN3 (Figure 3B). As a control, we confirmed that the combination of RU486 and DEX decreased the activation of the GR in both cell lines (Figure 3C). The involvement of the GR in increasing trafficking of R451C NLGN3 was also assessed by cytofluorimetric analysis on intact cells after the combined treatment with RU486 and DEX. We observed a reduced localization of R451C NLGN3 on the cell surface, compared with cells treated with DEX alone (Figure 3D). Taken together, these results indicate a direct involvement of the GR in mediating the effects of GCs, and in particular of DEX, on the cell surface trafficking of R451C NLGN3. We selected DEX for a detailed characterization of the effects of GCs in our cellular model of ASDs. First, we evaluated the effect of different concentrations and times of treatment on R451C NLGN3 protein levels and on the phosphorylation of the GR on Ser211. We observed a significant activation of the GR at all three tested concentrations of DEX (0.02, 0.2, and 2 μM, Figure 4A), as well as a similar increase in R451C NLGN3 protein levels (Figure 4B). An increase in the mutant protein levels was detectable only after 16 and 48 h of treatment with DEX at 2 μM (Figure 4C). However, the activation of the GR was observed from the earliest time point, with Ser211 phosphorylation detectable at similar levels at all time points (1, 8, 16, and 48 h; Figure 4D). DEX had no

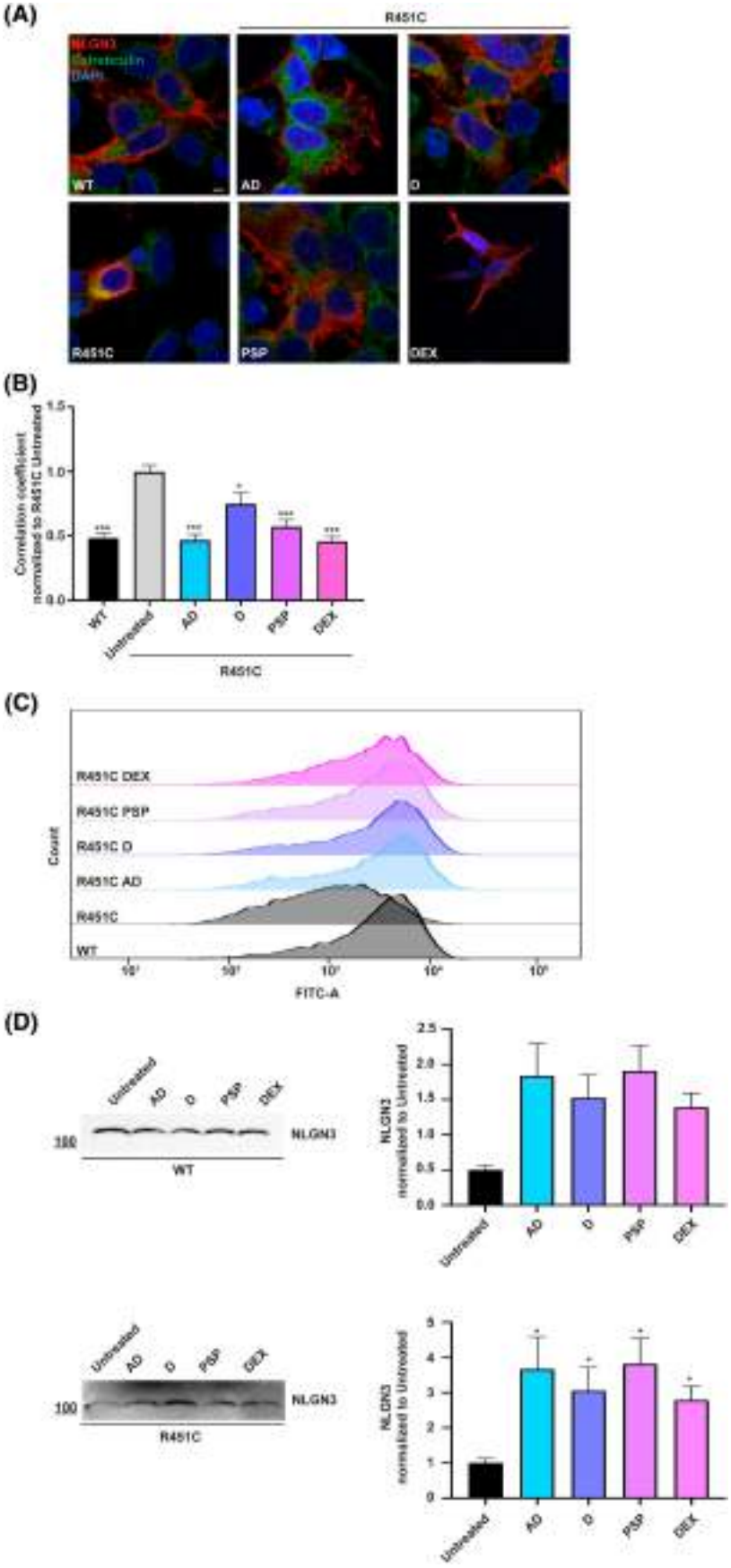

FIGURE 2 Selected glucocorticoids increase the trafficking of full-length NLGN3 to the cell surface. (A) Immunostaining of NLGN3 (red), the endoplasmic reticulum-resident protein calreticulin (green) and DAPI for nuclei visualization (blue) in HEK-293 expressing either wild type (WT) or R451C NLGN3. R451C NLGN3 expressing cells were either untreated or treated with the indicated compounds (2 μM for 48 h); scale bar: 1 μm. (B) Mander's overlap coefficient for NLGN3-calreticulin colocalization in cells expressing either WT or R451C NLGN3, treated and stained as in (A), normalized to untreated R451C NLGN3 cells (mean ± SEM; $n = 54$ cells/3 independent experiments; unpaired t-test $^{*}p < 0.05$, $^{***}p < 0.001$). (C) Flow cytometry analysis of surface NLGN3 in HEK-293 expressing either the WT or R451C NLGN3 protein. R451C NLGN3 expressing cells were either untreated or treated with the indicated compounds (2 μM for 48 h). (D) Representative western blots and densitometric analysis of NLGN3 levels in the culture media of HEK-293 cells expressing either WT or R451C NLGN3, untreated or treated with the indicated compounds (2 μM for 48 h; mean ± SEM; $n \geq 3$; unpaired t-test $^{*}p < 0.05$, $^{***}p < 0.001$). Compounds: AD, alclometasone dipropionate; D, desonide; DEX, dexamethasone; PSP, prednisolone sodium phosphate.

TABLE 2 FITC-A values in cells expressing WT or R451C NLGN3 following glucocorticoids treatments.

Population	Events	FITC-A mean
WT CTRL	9811	3677
R451C CTRL	10 758	1783
R451C AD	10 920	4038
R451C D	10 199	3875
R451C PSP	12 438	3844
R451C DEX	11 022	3015

Abbreviations: AD, alclometasone dipropionate; D, desonide; DEX, dexamethasone; PSP, prednisolone sodium phosphate; WT, wild type.

effect on NLGN3 protein levels in lysates expressing the WT protein, regardless of the concentration and time of treatment, although it was able to activate the GR at 2 μM (Figure 4B). Based on these results, we chose 2 μM and either 16 or 48 h as the best conditions for all subsequent experiments.

2.3 | DEX improves the stability of R451C NLGN3

We studied the decay of R451C NLGN3 protein over time by treating HEK-293 cells with the inhibitor of protein synthesis cycloheximide (CHX) for 24, 48, or 72 h. Treatment with CHX in combination with DEX significantly increased the levels of R451C NLGN3, both at 24 and 48 h, in comparison to CHX alone at the same time points (Figure 5A), suggesting that DEX enhances the stability of the mutant protein. Moreover, DEX treatment in combination with CHX increased the half-life of the mutant protein up to 55 h in comparison to CHX alone (23.4 h; Figure 5B). In order to understand whether DEX has a similar effect on other misfolded proteins, we transfected HEK-293 cells with a plasmid encoding for NLGN3 carrying the G221R substitution, previously characterized for causing a global misfolding of the protein and leading to its degradation through the proteasomal pathway.[29] DEX treatment had no effect on G221R NLGN3 protein levels compared with the untreated condition (Figure S1). Finally, we analyzed the effect of DEX on a mutant variant of the neuronal secretory protein neuroserpin, delta neuroserpin (ΔNS), which is detectable in the cell lysates only after treatment with the proteasomal inhibitor MG132.[31,32] Also in this case, treatment with DEX was not able to increase ΔNS protein levels compared with the untreated condition (Figure S1). These results suggest that DEX has an effect on the stability of only partially misfolded proteins.

2.4 | DEX reduces the ER stress induced by the R451C NLGN3 mutant protein

It was previously shown that R451C NLGN3 activates the UPR in vitro, in PC12 cells with inducible expression of mutant NLGN3,[23] and in vivo, in the cerebellum of the knock-in mouse R451C NLGN3.[21] Previous studies support a role for GCs in ameliorating UPR by enhancing the correct folding and secretion of proteins.[33,34] Based on this, we evaluated the effect of DEX on the levels of UPR sensors and mediators in our cell systems. We observed that DEX reduced the activation of protein kinase-like endoplasmic reticulum kinase caused by R451C NLGN3, as shown by the decrease in eIF2α phosphorylation in cells expressing mutant but not WT NLGN3 (Figure 6A). We also quantified the levels of the unprocessed form of activating transcription factor 6 (ATF6), which has been shown to be upregulated in ER stress conditions.[35] We found that DEX treatment reverted the increase in ATF6 levels observed in lysates of cells expressing R451C NLGN3, with no effect on WT NLGN3-expressing cells (Figure 6B). Finally, we analyzed the activation of the inositol-requiring enzyme 1 (IRE1) branch of the UPR by analyzing the downstream splicing of XBP-1, using a reporter plasmid expressing XBP1 fused to the fluorescent protein Venus. Under ER stress conditions, spliced XBP1 mRNA is translated into a fluorescent protein that can be detected by fluorescence microscopy.[36] As shown in Figure 6C, the treatment with DEX caused a reduction in the unconventional splicing of XBP1 in R451C NLGN3 cells, in comparison to the untreated cells. Among the target genes for the three UPR signaling cascades are several ER proteins such as immunoglobulin heavy-chain-binding protein (BiP), GRP94, and protein disulfide isomerase (PDI), involved in protein folding and ER quality control systems.[37] By analyzing the levels of these ER chaperones, we observed a decrease in PDI protein levels after treatment with DEX only in cells expressing R451C NLGN3, in agreement with the decrease in UPR activation (Figure S2A). However, DEX had no effect on the levels of GRP94 and BiP in either the WT or R451C NLGN3 cells (Figure S2B). These results show that DEX alleviates ER stress by modulating all three branches of the UPR and specific ER proteins.

2.5 | DEX increases synapse formation in cocultures with primary hippocampal neurons

It has been described that mutant R451C NLGN3 no longer has synaptogenic activity in vitro due to inefficient transport to the cell surface[18] and decreased affinity for the partner protein neurexin.[17] We next studied whether the treatment with DEX could rescue synapse formation. We analyzed the artificial synapses formed between HEK-293 cells, expressing NLGN3, and primary hippocampal neurons, cultured for 7 days before adding the HEK-293 cells. After 24 h, the cocultures were treated with 2 μM of DEX for 48 h. Immunofluorescence staining for the presynaptic marker VGLUT1 and NLGN3 (FLAG-staining) was followed by confocal microscopy analysis. As shown in Figure 7A, DEX treatment favored the formation of contacts between HEK-293 cells, either WT or R451C, and the neuronal synaptic terminals (Figure 7A), as shown by the increase in colocalization between VGLUT1 and NLGN3 on HEK-293 cells. These results were determined by assessing the proximity of VGLUT1 puncta to the

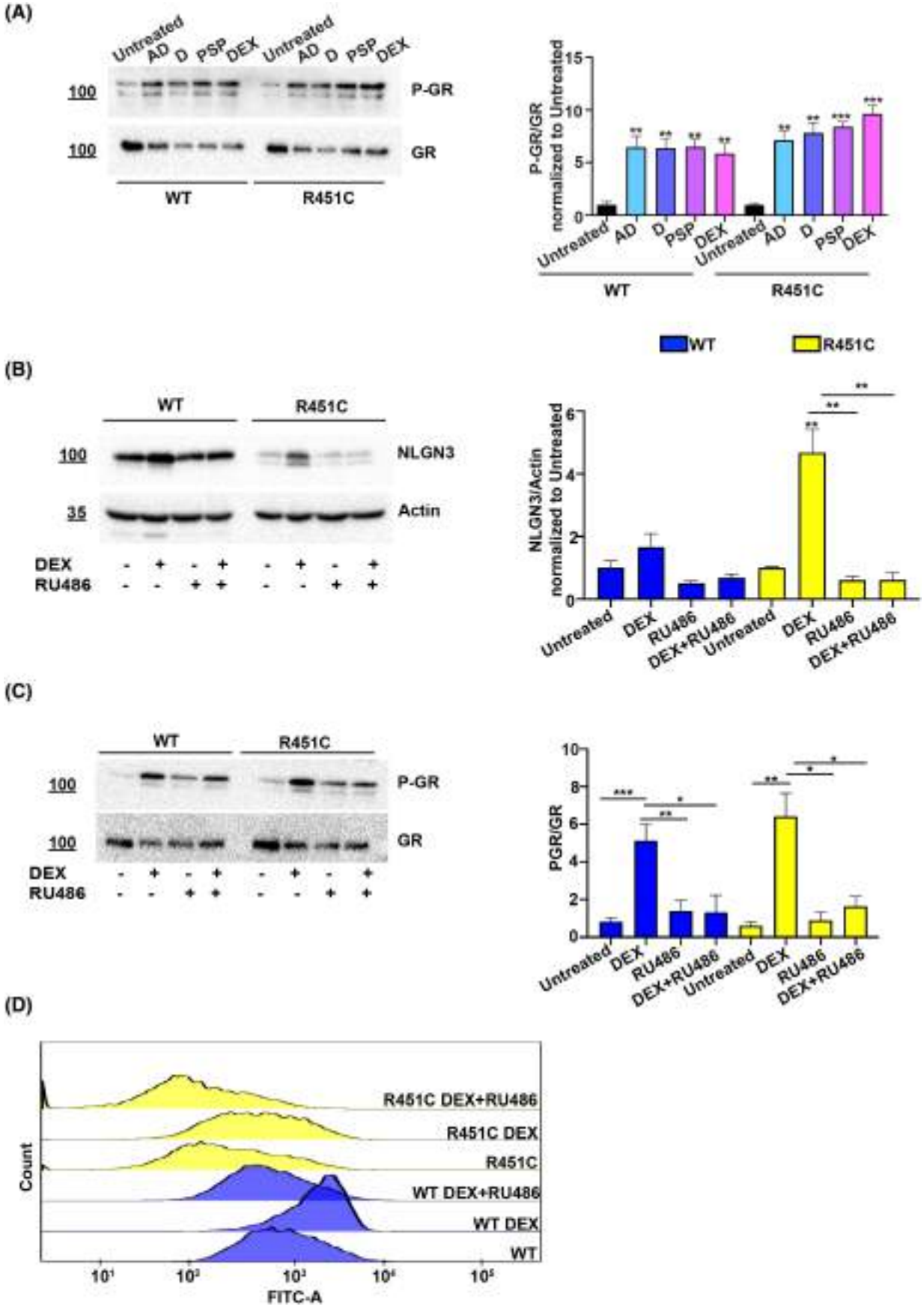

FIGURE 3 Legend on next page.

NLGN3 signal (FLAG-staining) after DEX treatment, compared with untreated cells (Figure 7A). It is noteworthy that DEX treatment led to a comparable level of colocalized signals in cocultures of hippocampal neurons with HEK-293 cells expressing either WT or R451C NLGN3. Notably, when comparing the distribution of colocalized signal areas in untreated cultures, we observed a more pronounced degree of colocalization in the WT cocultures as opposed to the mutant ones (Figure 7B).

As a control, we showed that DEX had no effect on VGLUT1 staining in primary neurons compared with untreated neurons, both in cocultures with WT NLGN3 cells (data not shown) and with R451C NLGN3 cells (Figure S3). Our results thus support that the increase in colocalization, in the presence of DEX, was not due to an increase in the number of presynaptic puncta but rather to the increased trafficking of NLGN3 to the cell surface.

2.6 | Generation of neural staminal progenitor cultures from adult mice brain

To validate the effects of DEX observed in HEK-293 cells overexpressing WT or R451C NLGN3, we derived NSPCs from the hippocampus of either WT or R451C NLGN3 adult male mice, according to protocols previously described.[38–40] When cultured under proliferative conditions, NSPCs express the staminal marker nestin, as confirmed by immunofluorescence analysis (Figure S4); while, after 15 days of culture in our differentiating conditions, differentiated NSPCs express the neuronal marker MAP2 (Figure S4). To validate our new model system, levels of NLGN1, 2, and 3 in proliferating and in differentiated conditions were analyzed both in WT and in R451C NLGN3 cells (Figure S5A). As expected, NSPCs derived from the hippocampus of R451C NLGN3 mice showed a strong reduction in NLGN3 protein levels compared with the WT cells as previously observed.[19,21,41] Moreover, mutant NLGN3 levels didn't increase after inducing differentiation (Figure S5A). We have previously shown that R451C NLGN3 is preferentially degraded by the proteasome, both in vitro and in vivo.[21,29] In agreement with this result, when R451C NLGN3 cultures were treated with the proteasome inhibitor MG132 (2 μM for 6 h), a significant increase in NLGN3 levels was observed, in comparison to the untreated condition (Figure S5B), confirming that the mutant protein is degraded by the proteasome in this newly generated system as well. No effect was observed in the NSPCs expressing WT NLGN3. For a detailed characterization of the physiological properties of the neuronal cultures at 15 days of differentiation, we studied the calcium flux in either WT or R451C NLGN3 differentiated cultures by evaluating the calcium transients evoked by a depolarizing stimulus, represented by a local application of 50 mM KCl. Endogenous calcium flux was visualized by loading either WT or R451C NLGN3 cells with Fluo4, a calcium-sensitive fluorescent dye.[42] R451C NLGN3 neurons showed a decreased amplitude after the KCl stimulus in comparison to WT neurons (Figure S5C), suggesting a different functional phenotype in comparison to WT cultures.

2.7 | DEX increases endogenous R451C NLGN3 levels, decreases UPR activation and increases the formation of synaptic puncta

Proliferating and differentiated NSPCs, derived from either WT or R451C knock-in mice, were treated with DEX (2 μM for 48 h). In line with our previous results, a significant increase in the R451C NLGN3 protein levels was observed after DEX treatment in both proliferating and differentiated conditions, while no effect was found in cells expressing the WT protein (Figure 8A,B). To assess whether the increase in the R451C NLGN3 levels elicited by DEX in NSPCs lysates in proliferative conditions was due to a transcriptional regulation, the mRNA for NLGN3 was quantified by real-time polymerase chain reaction (RT-PCR). No changes were found in the relative amounts of either R451C or WT NLGN3 mRNA after DEX treatment in comparison to the untreated conditions (Figure S6), supporting a post-translational effect caused by the compound on the stability of the mutant protein. In agreement with our published data, proliferating and differentiated cultures expressing R451C NLGN3 showed higher levels of the chaperone BiP in comparison to WT cultures (Figure 8C,D).[21,23] Interestingly, DEX treatment decreases BiP levels in NSPCs expressing R451C NLGN3, demonstrating a reduction of the UPR that is not detectable in WT cultures (Figure 8C,D). Since our previous results in HEK-293 cells showed that higher levels of NLGN3 on the cell surface were able to induce artificial synapses by recognizing the presynaptic partner protein, we decided to analyze the expression of Synapsin1, a marker of synaptic specialization.[43,44] Our data indicate that the number of synaptic puncta increases after DEX treatment in both WT and R451C NLGN3 differentiated NSPCs cultures (Figure 9).

FIGURE 3 The activation of the glucocorticoid receptor (GR) is responsible for the stabilization of intracellular R451C NLGN3 caused by dexamethasone (DEX) treatment. (A) Representative western blot and densitometric analysis of phosphorylated GR levels in either wild type (WT) or R451C NLGN3 expressing cells after treatment with alclometasone dipropionate (AD), desonide (D), DEX or prednisolone sodium phosphate (PSP; 2 μM for 48 h), normalized to total GR and to the corresponding untreated condition (mean ± SEM; $n = 3$; unpaired t-test; $^{**}p < 0.01$, $^{***}p < 0.001$). (B) Densitometric analysis and representative western blot of NLGN3 levels in lysates from WT and R451C NLGN3 expressing cells either untreated or treated with DEX (2 μM for 48 h), RU486 (20 μM for 48 h) or both compounds, normalized to the corresponding untreated condition (mean ± SEM; $n = 3$; unpaired t-test; $^{**}p < 0.01$). (C) Representative western blot and densitometric analysis of phosphorylated GR (P-GR) and total GR levels in lysates from WT and R451C NLGN3 expressing cells untreated or treated with DEX (2 μM for 48 h), RU486 (20 μM for 48 h) or both compounds (mean ± SEM; $n = 3$; unpaired t-test $^{*}p < 0.05$, $^{**}p < 0.01$, $^{***}p < 0.001$). (D) Flow cytometry analysis of surface NLGN3 in HEK-293 expressing either WT or R451C NLGN3, untreated or treated with DEX (2 μM for 48 h) or with a combination of DEX and RU486 (RU486 20 μM for 48 h) as indicated.

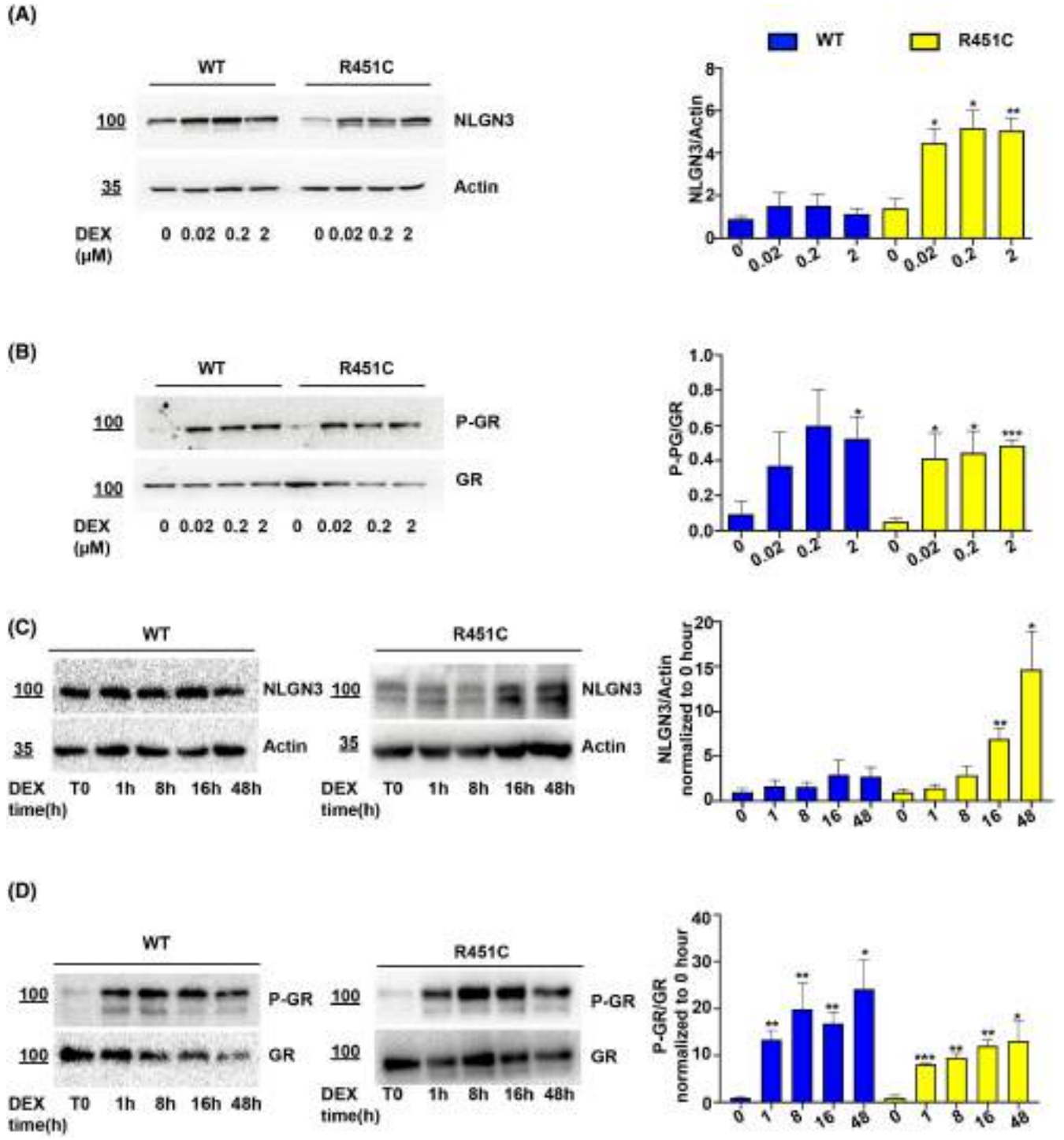

FIGURE 4 Dose–response and time-course analysis of dexamethasone (DEX) effects on NLGN3 protein levels and glucocorticoid receptor (GR) activation. (A) HEK-293 stably expressing full-length NLGN3, either wild type (WT) or R451C, were untreated (0) or treated with DEX at different concentrations (0.02, 0.2, or 2 μM) for 48 h and cell lysates were analyzed by western blot for NLGN3 normalized to actin (B), western blot analysis for phosphorylated GR (P-GR) and total GR levels, followed by densitometric analysis. HEK-293 stably expressing full-length NLGN3, either WT or R451C, were treated with DEX 2 μM for different hours (0, 1, 8, 16, and 48) and cell lysates analyzed by western blot for NLGN3 (C, normalized to 0 h; D) western blot analysis for phosphorylated GR (P-GR) and total GR levels, normalized to 0 h, followed by densitometric analysis. Results are expressed as the mean ± SEM; $n = 3$; unpaired t-test $^{*}p < 0.05$, $^{**}p < 0.01$.

3 | DISCUSSION

Cell adhesion presynaptic and postsynaptic proteins, including the NRXNs and the NLGNs, have a role in the maturation, function, and specification of the synapse.[8] Alterations in protein processing and cell surface trafficking of the NLGNs have been described for several ASDs-associated mutations, mainly deriving from amino acid substitutions causing misfolding of the extracellular domain in the

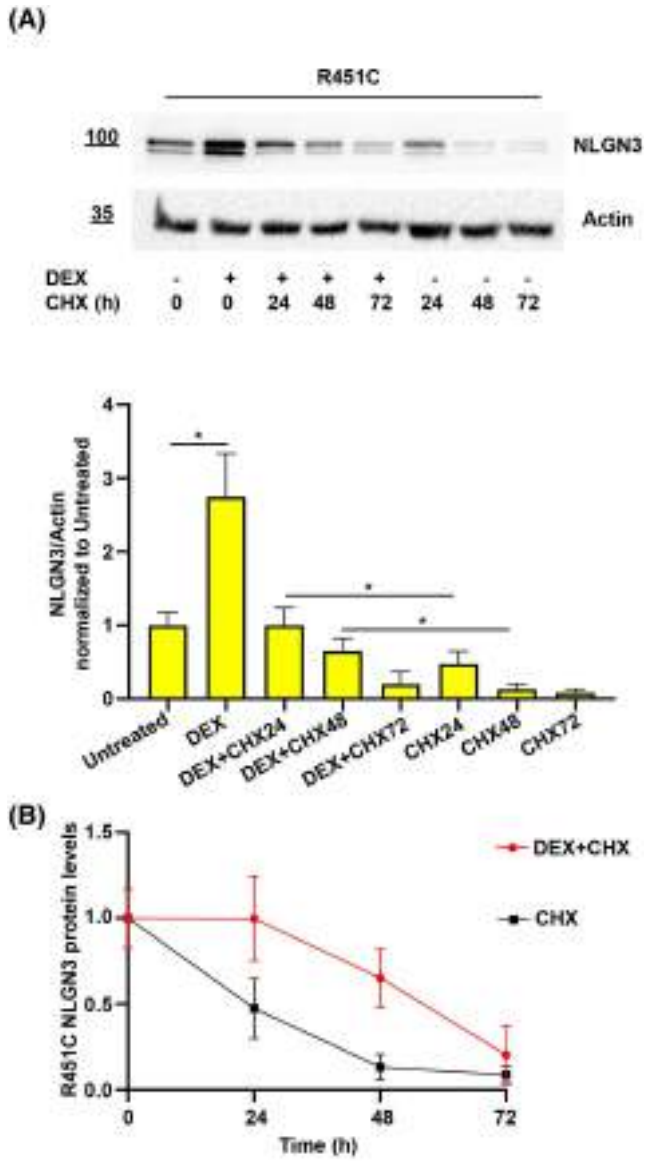

FIGURE 5 Dexamethasone (DEX) treatment stabilizes the intracellular R451C NLGN3 protein. (A) HEK-293 cells expressing R451C NLGN3 were treated with cycloheximide (CHX, 70 μM) in the presence or absence of DEX (2 μM) for the times indicated in the figure. The figure shows a representative western blot analysis of the cell lysates and the quantification of NLGN3 R451C bands by densitometry, normalized to actin and the untreated condition (mean ± SEM; $n = 3$; unpaired t-test $^*p < 0.05$). (B) Band intensities of the three experiments in (A) were quantified and normalized to the corresponding untreated condition to obtain the curves representing the degradation rates in the presence or absence of DEX; from these curves, the half-life of R451C NLGN3 was calculated as 23.4 h without DEX and 55 h with DEX.

NLGN3 and NLGN4 proteins.[4] While some of the mutations severely disrupt the structural integrity of the extracellular neurexin-binding domain, others result in milder effects depending on the region they map in the structure.[45] Among all the mutations found in the NLGNs, the R451C NLGN3 was the first to be identified in ASDs patients and it represents the reference mutation in the field because it has been extensively studied by our and several other groups over two decades.[9,21,23,29] The R451C substitution causes a localized misfolding of the extracellular domain of NLGN3, which is therefore significantly retained in the ER with only a residual fraction of the protein reaching the cell surface.[19,29,46] Although this mutation has been highly characterized for its effects in several model systems both in vitro and in vivo, few studies attempted to identify a possible rescue strategy for correcting impaired cell surface trafficking. For this reason, we have generated a simple but reliable cell system expressing a truncated and fluorescent form of R451C NLGN3 and screened an FDA-approved library of 2662 small chemical compounds. We identified 13 compounds able to increase the secretion of the truncated R451C NLGN3 in the culture medium[17,28,29,47] and we initially studied the effects of four of them (AD, D, PSP, and DEX), all belonging to the GCs family. We showed that they caused increased levels of full-length R451C NLGN3 but did not affect levels of NLGN3 in cells expressing the WT form of the protein. With this analysis, we quantified total protein levels in the cells, including the fractions undergoing the maturation process, retained in the ER, and exposed on the cell surface. On the contrary, using fluorescence activated cell sorting (FACS) analysis on intact cells, we specifically measured the amount of protein exposed on the cell membrane and our results clearly showed that all compounds increased levels of both WT and mutant protein reaching the cell surface, thus having an effect in promoting the overall trafficking of NLGN3. In line with these results, we showed by immunocolocalization staining, that all four tested GCs were able to favor the exit of the R451C protein fraction retained in the ER. Generally, NLGN3 performs its functions tethered to the cell membrane, although it has been recently shown that its extracellular domain can be cleaved and secreted in the medium to regulate physiological processes, such as cell proliferation in glioma.[48,49] The presence of ASDs-linked mutations specifically impairing folding and cell surface trafficking of NLGN3, also reduced the extracellular levels of the cleaved form in the culture medium.[24] As expected, in our model system of HEK-293 cells stably overexpressing R451C NLGN3, we observed reduced levels of the cleaved protein form in the culture medium in comparison to cells expressing the WT protein, as previously observed by Quartier et al.[24] More interestingly, treatment with the four GCs led to a higher amount of cleaved R451C extracellular domain in the culture medium. This result indirectly supports an effect of the treatment in enhancing trafficking of the mutant protein from the ER to the cell surface.

To simplify the study, we continued our analysis of the molecular mechanisms elicited by the GCs, by using only one of the four compounds. Hence, DEX was chosen for its documented ability in promoting cell surface trafficking of other proteins in in vitro cellular systems.[50,51] Moreover, the use of this drug offers the translational value of using it in in vivo studies. Nonetheless, the effect of DEX on protein trafficking has never been approached in the study of a synaptic protein or in the contest of ASDs.

Our results showed that DEX treatment prolonged the half-life of the mutant protein, from 23.4 to 55 h, therefore improving its stability. The effect of DEX may be related to the local nature of the

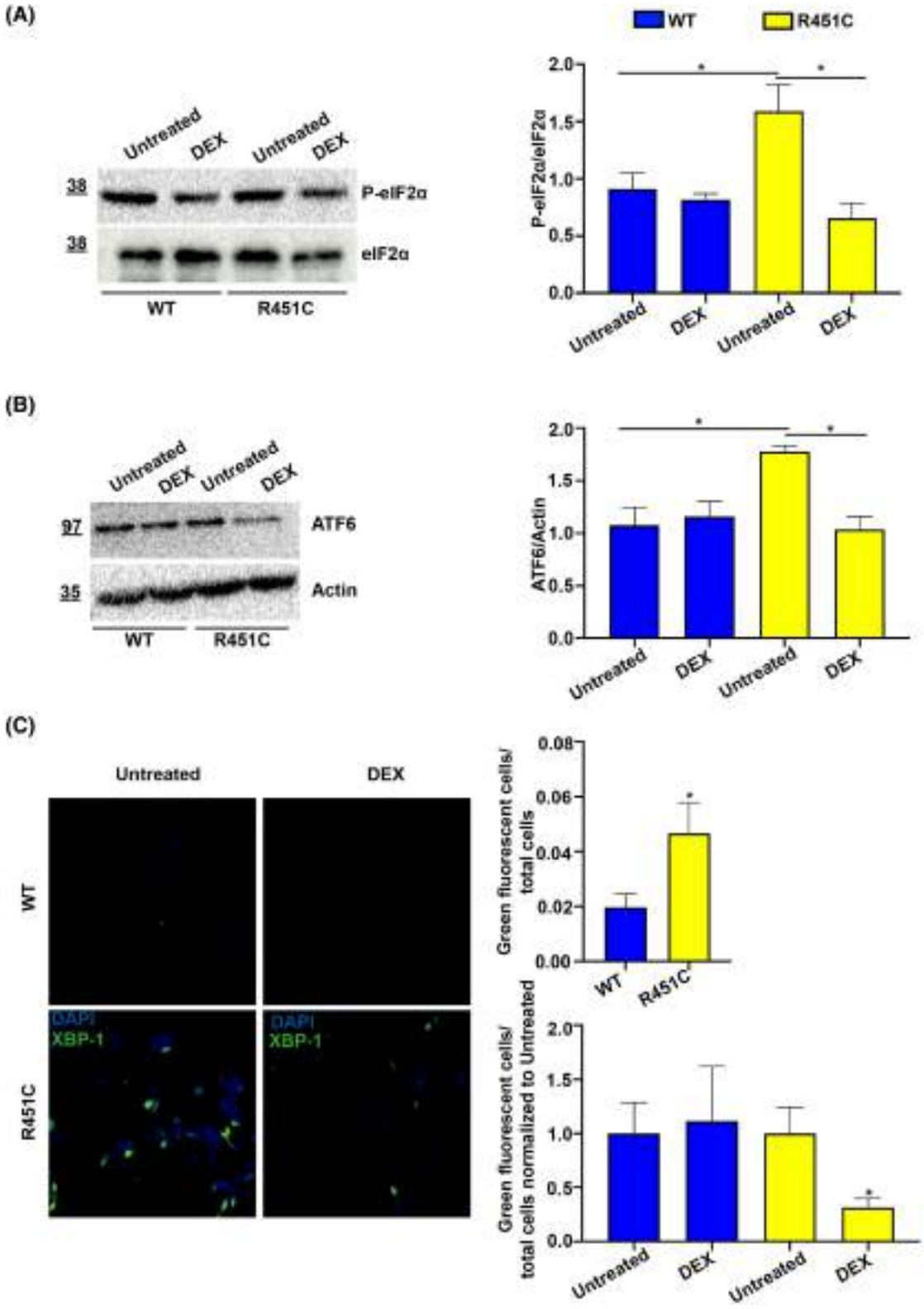

FIGURE 6 Dexamethasone (DEX) treatment reduces the activation of the three branches of the unfolded protein response (UPR). (A) Representative western blot and densitometric analysis of phosphorylated eIF2α (P-eIF2α) normalized to total eIF2α levels in the lysates of wild type (WT) or R451C NLGN3 expressing cells, either untreated or treated with DEX (2 μM for 48 h; mean ± SEM; $n = 3$; unpaired *t*-test $^*p < 0.05$). (B) Representative western blot and densitometric analysis of ATF6 protein levels in the lysates of WT or R451C NLGN3 expressing cells, either untreated or treated with DEX (2 μM for 48 h), normalized to actin (mean ± SEM; $n = 3$; unpaired *t*-test $^*p < 0.05$). (C) Detection of spliced XBP1 by using a fluorescence reporter (pCAX-F-XBP1ΔDBD-Venus, green) transiently expressed in WT or R451C NLGN3 cells, either untreated or treated with DEX (2 μM for 48 h). DAPI (blue) was used to stain the nuclei. The histograms show the ratio between green fluorescent cells (spliced XBP1) and total cells (DAPI) normalized to the untreated condition (mean ± SEM; $n = 4$; unpaired *t*-test $^*p < 0.05$).

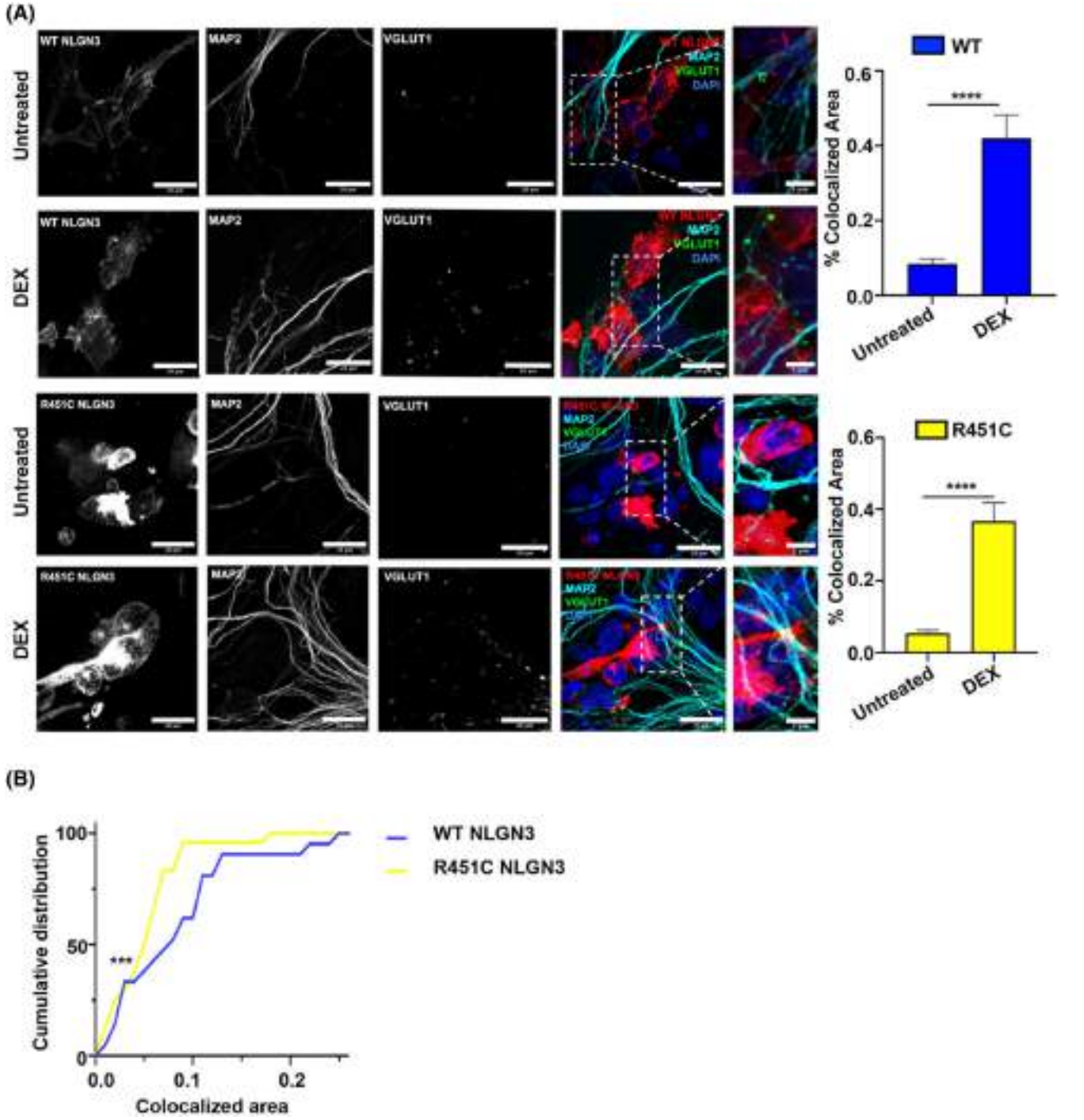

FIGURE 7 Dexamethasone (DEX) treatment enhances the number of synapses in cocultures of hippocampal neurons and HEK-293 cells expressing wild type (WT) or R451C NLGN3. (A) Representative confocal immunofluorescence images of NLGN3-FLAG (red), MAP2 (cyan), and VGLUT1 (green) staining of cocultured hippocampal neurons and HEK-293 cells expressing WT or R451C NLGN3, untreated or treated with DEX (2 μM for 48 h; scale bar: 20 μm, DAPI for nuclei visualization in blue). The inserts are zoomed images showing the neuronal presynaptic protein VGLUT1 on the surface of HEK-293 cells expressing WT or R451C NLGN3 (scale bar: 5 μm). The images show a maximum intensity projection of a region of interest. The histograms show the quantification of NLGN3 and VGLUT1 colocalization, expressed as the percentage of VGLUT1 puncta in proximity to the HEK-293 area. Values are expressed as mean ± SEM ($n = 11$ fields from three independent experiments; Mann Whitney $^{****}p < 0.0001$). (B) The graph illustrates the cumulative distribution of colocalized area for untreated WT (blue) and R451C NLGN3 (yellow) cocultures. Statistical significance was assessed by the Kolmogorov Smirnov test ($^{***}p < 0.001$).

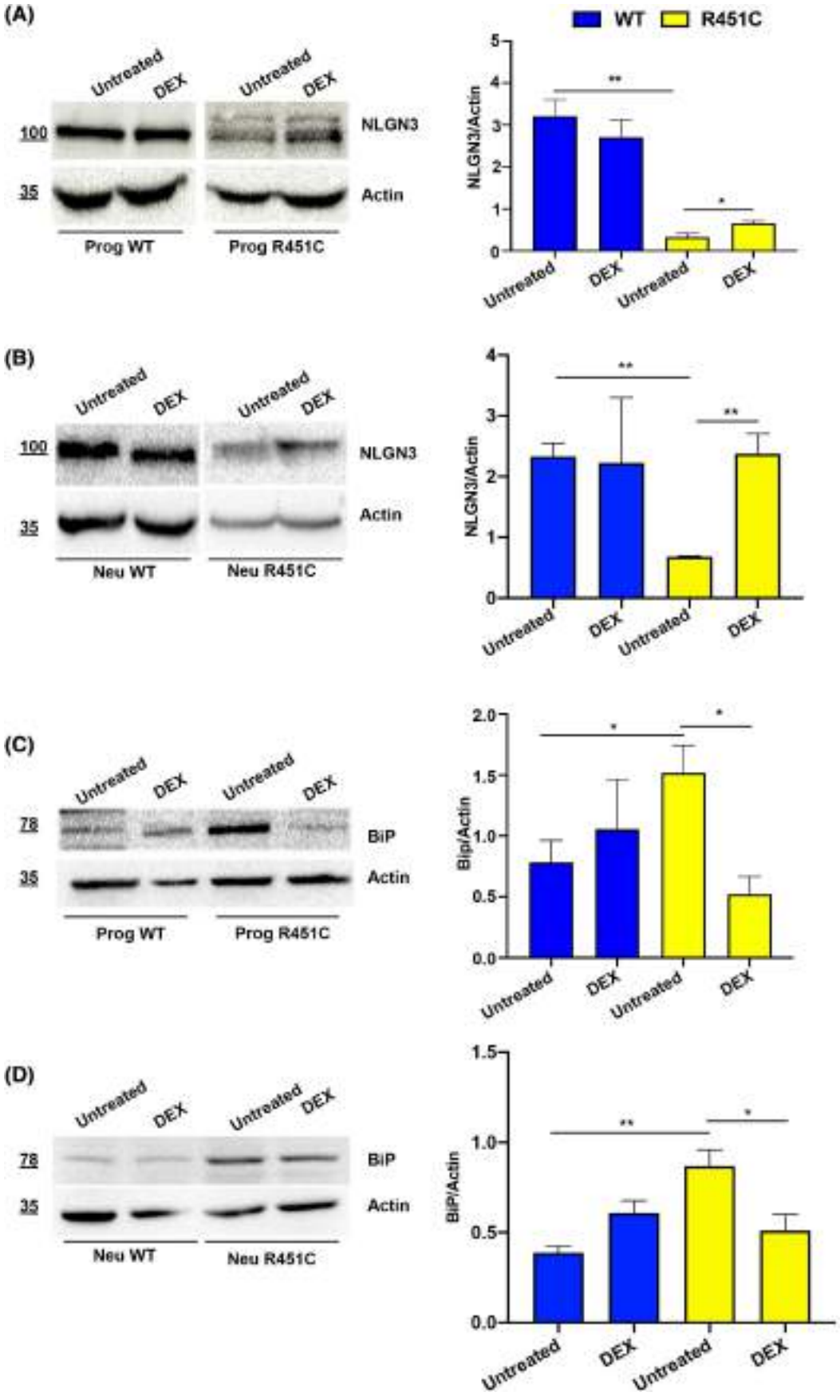

FIGURE 8 Legend on next page.

misfolding caused by the R451C mutation in the NLGN3 structure (De Jaco et al., 2010). In fact, DEX had no effect on improving trafficking of other misfolded neuronal proteins such as a mutant form of neuroserpin (Δneuroserpin) or NLGN3 protein carrying a more severe mutation (G221R). This is probably due to the severity of the defect introduced by these mutations in the respective protein structure.[29] Moreover, the increased protein levels and trafficking of mutant NLGN3 to the plasma membrane are abolished when mifepristone (RU486), an antagonist of the GR receptor, is supplemented to the cell medium in combination with DEX, supporting a direct involvement of the signaling activated by this receptor in the rescue of the R451C NLGN3 trafficking.

The dual genetic and environmental nature characterizing ASDs represent the main obstacle to the search for effective therapies.[52] However, many pharmacological therapeutic approaches have been developed to modulate UPR effectors. Our group has previously shown that the retention of R451C NLGN3 causes ER stress and the activation of the UPR both in vitro and in vivo, which is correlated to neurotransmission alterations in the cerebellum.[21,23] Several studies provide support for a protective effect of GCs on ER stress and UPR, both directly and indirectly.[33,34,53–57] Our results showed that DEX treatment in HEK-293 cells stably over-expressing the autism-linked mutant R451C NLGN3, decreased the levels of mediators (EIF2alpha, ATF6, and XBP-1) downstream the main branches of the UPR, repristinating the homeostasis in the ER. Furthermore, the analysis of UPR targets showed decreased levels of PDI, which plays a crucial role in protein folding by catalyzing disulfide bond formation.[58]

To understand whether the greater fraction of R451C NLGN3 protein present on the cell surface following DEX treatment, was able to interact with the physiological partner neurexin, we analyzed the formation of artificial contacts between HEK-293 overexpressing NLGN3 and primary hippocampal neurons. Our experiments showed a higher number of contacts after treating the cocultures with DEX, in comparison to the untreated control. This suggests that the fraction of protein reaching the cell surface is able to interact with neurexin despite the presence of the mutation. However, the effect of DEX does not seem to be specific for the R451C mutation, since it also increases the formation of artificial synapses between hippocampal neurons and HEK-293 cells expressing the WT form of NLGN3. These results are probably correlated to the increased trafficking of WT NLGN3 to the cell surface shown by the FACS analysis. Indeed, since NLGN3 is a cell-adhesion protein, higher amounts of the protein on the cell membrane lead to an increased number of synaptic contacts.

To validate our results in a physiological cell system, we chose to use NSPCs derived from the hippocampal region of adult knock in mice endogenously expressing the R451C mutation.[19] NSPCs are advanced cell cultures for studying neurodevelopmental disorders, including ASDs and a valuable tool for studying cellular mechanisms underlying the effect of potential therapeutic drugs.[59] NSPCs cultures express R451C NLGN3 as the endogenous protein and the regulation of the gene is under the proper gene promoter. We also derived NSPCs from the murine parental strain, as a control. WT NLGN3 was correctly synthesized and expressed in both proliferative and differentiated conditions, while the cultures expressing R451C NLGN3 showed poorly detectable levels of mutant NLGN3, thus reproducing the trafficking defects described in previous in vitro systems and in the in vivo knock in mouse model.[23,29] On the contrary, NLGN1 and 2 protein levels were normal and progressively increased during neuronal differentiation in both WT and R451C NLGN3-expressing cells. NSPCs cultures expressing R451C NLGN3 showed UPR activation as demonstrated by higher levels of the UPR target BiP in comparison to WT, in line with what we have previously observed in other in vitro and in vivo systems.[21,23] Moreover, the R451C NLGN3 cultures showed a slower calcium response after depolarization, in comparison to the WT cells. This is in agreement with the dysregulation of Ca^{2+} concentration that is associated with several neurodevelopmental disorders, including ASDs.[60] Treatment of NSPCs cultures expressing endogenous R451C NLGN3, with DEX, improved mutant protein levels, both in proliferative and differentiated conditions, confirming the results obtained in the HEK-293 cells. Moreover, the drug decreased the ER stress by reducing the levels of BiP and therefore repristinating the homeostasis in the ER. Although UPR mediators are reduced in both cell model systems, the decrease of the UPR-target gene BiP was only observed in the lysates from NSPCs cultures but not in the lysates of HEK-293 over-expressing the mutant protein. This could reflect a higher sensitivity of the NSPCs, where the endogenous mutant protein has a higher impact on the cellular homeostasis and the effect of DEX results in a stronger outcome. Unfortunately, it was not possible to evaluate whether DEX increased the localization of endogenous NLGN3 on the cell surface, therefore favoring the formation of synaptic contacts in differentiated cultures expressing R451C NLGN3, since the endogenous protein is not flag-tagged and there are no commercially available antibodies against NLGN3 to be used in immunostaining. However, to overcome this limitation, we analyzed the number of Synapsin 1 puncta in differentiated cultures and found that the presynaptic protein increased after DEX treatment in both genotypes, suggesting the formation of a higher number of synaptic contacts.

In this work, we present a novel cellular model of an ASDs-related mutation that recapitulates the effects of the R451C substitution in NLGN3 and allows us to study the molecular mechanisms linked to a monogenic form of ASDs in physiological conditions since the

FIGURE 8 Dexamethasone (DEX) treatment increases R451C NLGN3 endogenous protein levels and reduces UPR activation in proliferating and differentiated neural stem progenitor cells (NSPCs). (A,B) Representative western blot and densitometric analysis of NLGN3 levels (normalized to actin) in proliferating (A) or differentiated for 7 days (B, Neu) NSPCs expressing endogenous wild type (WT) or R451C NLGN3, treated or not with DEX (2 μM for 48 h; mean ± SEM; $n = 3$; unpaired t-test $^{*}p < 0.05$, $^{**}p < 0.01$). (C,D) Densitometric analysis and representative western blot of BiP protein levels (normalized to actin) in proliferating (C) or differentiated for 7 days NSPCs expressing endogenous WT or R451C NLGN3 treated or not with DEX (2 μM for 48 h; mean ± SEM; $n = 3$; unpaired t-test $^{*}p < 0.05$).

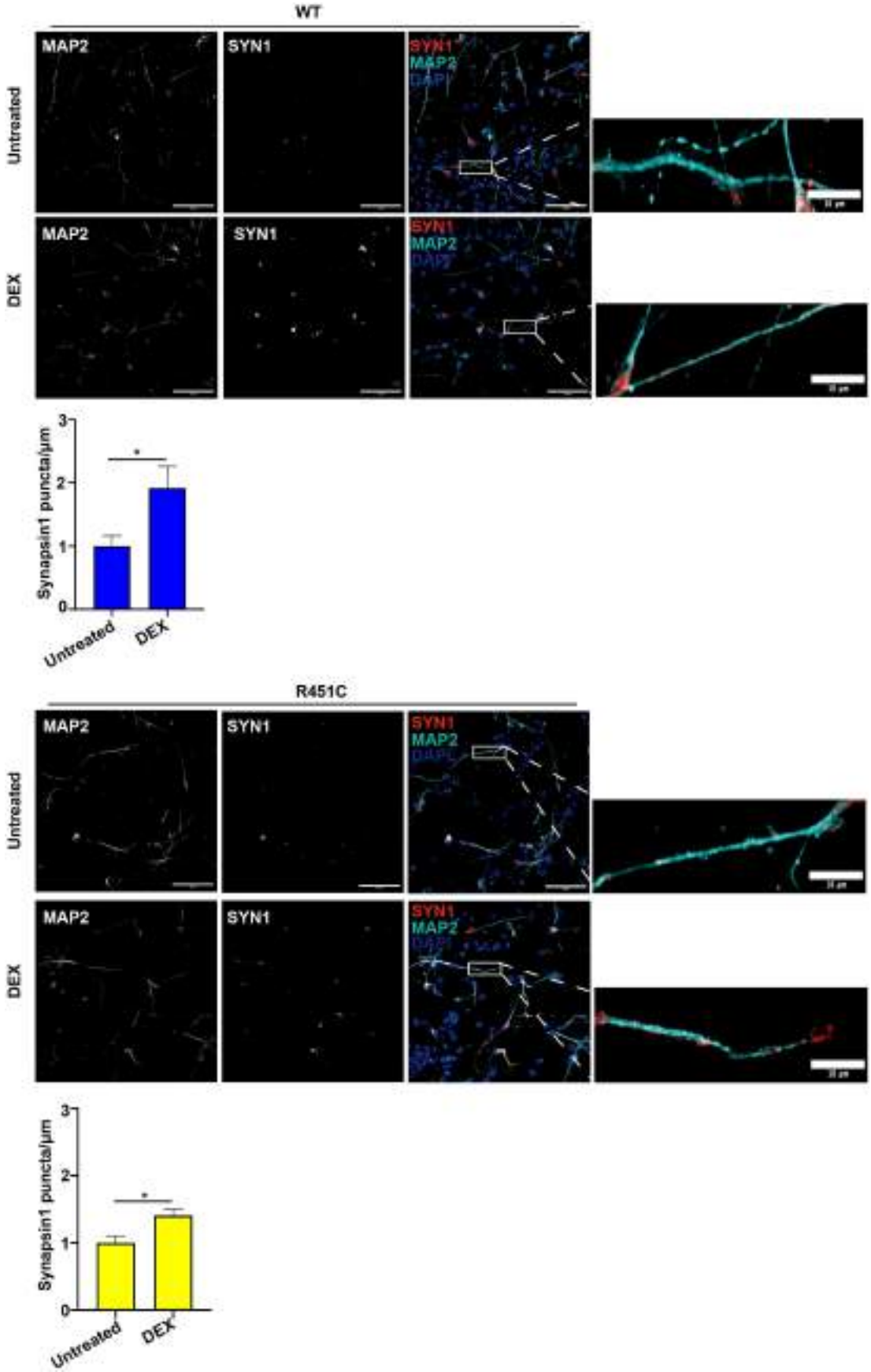

FIGURE 9 Legend on next page.

expression of the mutant protein is endogenous. Moreover, our results indicate that the treatment with DEX is a valuable approach to increase the stability of R451C NLGN3 and promote its trafficking to the cell membrane, where it can play its role in inducing the formation of synaptic contacts.

This work is part of a new and intriguing field of research, which aims to find possible strategies to improve altered protein trafficking for diseases correlated with protein misfolding, most of which have been untreatable so far. The use of FDA-approved GCs could enhance the secretion of proteins and alleviate the UPR in different cell systems, as we show here for a mutant variant of NLGN3 both in overexpression and in endogenous conditions. Moreover, our work shows and confirms that the use of GCs may be beneficial to many forms of human disease involving protein misfolding and ER stress.[33] In summary, this study shows a potential strategy to reduce the accumulation of misfolded proteins in the ER, enhancing surface trafficking, secretion, and synapse formation. If these effects translate in vivo, these drugs may have positive effects in contrasting the pathological processes of neurodevelopmental disorders caused by genetic mutations related to ASDs.

4 | MATERIALS AND METHODS

4.1 | Transient transfection

HEK-293 cells were transfected using poly-ethylenimine (PEI; Sigma–Aldrich-Merck, Milano, Italy). Cells were seeded in a 6-well plate and transfected, the day after the seeding, with the pcDNA3.1 plasmid encoding full-length NLGN3 WT, NLGN3-R451C, or NLGN3-G221R. Alternatively, HEK-293 cells were transfected using a pTP6-NS plasmid encoding for ΔNS.

4.2 | Stable transfection and clonal selection

HEK-293 cells were stably transfected using the pcDNA3.1 plasmid encoding full-length NLGN3, either WT or R451C, or the pcDNA3.1 plasmid encoding the extracellular domain of NLGN3-Venus either WT or carrying the R451C mutation.[17,28,29,47] Transfected cells were cultured in a selective medium composed by Dulbecco's Modified Eagle's Medium, 5% fetal bovine serum (FBS; Sigma-Aldrich), and 500 μg/mL Geneticin (G418, Corning). Resistant cells were plated at clonal density in 96-well plate and expanded to obtain clones, which were screened for NLGN3 protein expression by western blot on cell lysates or media. Stable cell lines were maintained at 37°C and 5% CO_2 in the presence of G418.

4.3 | Cell treatments

AD, D, DEX, or PSP were added in the cell culture medium 24 h after seeding. All tested compounds were dissolved in 100% dimethyl sulfoxide (DMSO) at the concentration of 3.84 mM, except for DEX which was prepared at a concentration of 50 μM and added in the cell culture medium at the final concentration of 2 μM for 48 h. In the dose/response experiments the final concentrations tested were 0.02, 0.2, and 2 μM. CHX (at concentration 70 μM) was added to the cell culture medium for 24, 48, or 72 h. The GR antagonist mifepristone (RU486, at concentration 20 μM) was added to the cell culture medium for 48 h. The proteasome inhibitor MG132 (at concentration 2 μM) was added to the cell culture medium for 16 h (Z-Leu-Leu-Leu-al, no. C2211 Sigma–Aldrich).

4.4 | Screening of the FDA-approved compounds

For the screening of FDA-approved compounds, we used stable HEK-293 cell lines expressing a truncated and fluorescent form of NLGN3 (NLGN3-Venus), either WT or R451C. Cells were plated at a density of 75000 cells in 96-well plate, in 150 μL Optimem medium added with 2% FBS.

The compounds of the library were dissolved in 10% DMSO (Sigma-Aldrich) in H_2O and used at the final concentration of 2 μM. Compounds were added in the cell culture medium 24 h after seeding and fluorescence levels were measured after 60 h of treatment.

4.5 | Quantification of protein secretion by fluorimetric measurement

NLGN3-Venus protein trafficking was evaluated by transferring 100 μL of medium from cells either untreated or treated with selected compounds in a black 96-well plate and fluorescence was measured with the Promega Glomax fluorometer (excitation wavelength 485 nm, emission wavelength 535 nm).

4.6 | Mouse genotyping

B6;129-Nlgn3tm1Sud/J knock-in mice (R451C) and parental strain (WT) were a kind gift from Dr. Andrea Barberis (Italian Institute of Technology, Genova). All experimental procedures were done on littermate mice, obtained from mating either WT or R451C (knock-in) male mice with heterozygous females. Mice were provided with ad lib

FIGURE 9 Dexamethasone (DEX) treatment increases Synapsin 1 puncta in differentiated neural stem progenitor cells (NSPCs). Representative images of MAP2 (cyan) and Synapsin 1 (red) of wild type (WT) or R451C NLGN3 differentiated cultures, untreated or treated with DEX (2 μM for 48 h; scale bar: 50 μm, DAPI for nuclei visualization in blue). The images show a maximum intensity projection of a region of interest. Synapsin 1 puncta was counted within MAP2-positive segments of 50 μm. The analysis was performed on 10 segments (mean ± SEM; $n = 5$ fields of three independent experiments; unpaired t-test $^{*}p < 0.05$, $^{**}p < 0.01$). The inserts are zoomed images showing the Synapsin 1 puncta localized on MAP2 positive neurites (scale bar: 10 μm).

food and water and were kept on a 12-h light/12-h dark cycle at the temperature of 20 ± 1°C. The experiments were done on 2-month-old mice (P60) mice. For genotyping, the R451C mutation was detected after PCR amplification of the genomic DNA, extracted from the mouse tail using primers previously described.[19] The DNA was used for PCR amplification of the insertion site of the loxP site in the NLGN3 gene (FW 5′-TGTACCAGGAATGGGAAGCAG-3′; RW 5′-GGTCAGAGCTGTCATTGTTCAC-3′). Amplified DNA shows a 40 bp size shift for the R451C-NLGN3 genomic DNA in comparison with WT. Mouse sacrifice was done according to the animal protocol and to the current Italian law (D.lgs. 26/2014). All experimental procedures and protocols were approved by the Ethical Committee for Animal Research of the Italian Ministry of Public Health (Authorization N. 541/2016-PR; 351/2021-PR).

4.7 | NSPCs cultures and culture media

NSPCs were obtained from the dentate gyrus of 2-month-old WT and R451C knock-in male mice and expanded as previously described.[38–40,61,62] After dissection of dentate gyrus, the tissues were collected in Leibovitz's L-15 medium, mechanically dissociated, and resuspended in HBSS (Gibco) containing 5.4 mg/mL D-glucose, 18 mM Hepes, 0.74 mg/mL trypsin, 200 U/mL DNase, 0.7 mg/mL hyaluronidase, and 2 mg/mL kynurenic acid (all from Sigma) pH 7.5 and digested for 20 min at 37°C. Living cells were counted by using the trypan blue exclusion method and plated in uncoated plastic flasks at 5×10^4 cells/mL density. Very small neurospheres appeared as early as 4–5 days; neurospheres were grown until they reached medium size (roughly 100–150 μm), and then collected, enzymatically dissociated, and plated on Poly-Ornithine/laminin-coated flasks. Adherent NSPCs were routinely cultured in expansion medium constituted by DMEM/F12, supplemented with 1% penicillin/streptomycin, 0.1 M L-glutamine (Gibco), 23.8 mg/100 mL Hepes, 7.5% $NaHCO_3$, 0.6% glucose, 20 ng/mL human recombinant EGF (Peprotech), 10 ng/mL bFGF (Peprotech), and 0.5% B-27™ Supplement (50×), serum-free supplement (Gibco).

NSPCs were cultured in adherent condition on Poly-Ornithine (10 μg/mL, Sigma) and laminin (5–2.5 μg/mL, Corning) coated flasks or coverslips and maintained under proliferative conditions at 37°C in a 5% CO_2 atmosphere, half of medium was replaced with fresh medium each 3 days.

NSPCs were differentiated according to previously established protocols.[27,39] The differentiation media consist of: DMEM/F12, 1% penicillin/streptomycin, 0.1 M L-glutamine (Gibco), 23.8 mg/100 mL Hepes, 7.5% $NaHCO_3$, 0.6% glucose, containing 0.5% B-27™ Supplement (50×), serum-free supplement (Gibco), with increasing dose of brain-derived neurotrophic factor (BDNF) (from 20 to 30 ng/mL, Peprotech) and decreasing dose of bFGF (from 10 to 5 ng/mL, Peprotech). For initial differentiation, the NSPCs cultures were exposed to a medium composed of DMEM/F12 medium (Invitrogen), containing 0.5% B-27™ Supplement (50×), serum-free supplement (Gibco), and supplemented with bFGF-2 (10 ng/mL; PeproTech, Tebu-Bio) and BDNF (20 ng/mL; PeproTech, Tebu-Bio) and cultured for 3 days at 37°C. For terminal differentiation, the cultures were exposed to a medium composed of a 1:3 mix of DMEM/F12 and neurobasal media containing 0.5% B-27™ Supplement (50×), serum-free supplement (Gibco) and containing bFGF-2 (5 ng/mL), BDNF (30 ng/mL) and sodium pyruvate 1 mM. The cells were maintained for an additional 7–15 days; the medium was changed every 3 days.

4.8 | Immunocytochemistry of NSPCs and differentiated cultures

Cells were fixed with 2% PFA in phosphate buffered saline (PBS) for 5 min and then with 4% PFA for 15 min. After fixation, cultures were washed with potassium-PBS (KPBS), pH 7.4, and then incubated in KPBS containing 5% of the appropriate normal serum and 0.025% Triton X-100 (preincubation solution) for 1 h at room temperature. Subsequently, cultures were incubated at 4°C overnight in a preincubation solution containing the following primary antibodies: anti-Nestin (Millipore, MAB5326 1:500), anti-MAP2 (chicken, 1:200, Abcam ab5392), anti-Synapsin 1 (Cell Signaling, D12G5, 1:200). Secondary antibodies were incubated for 1 h at room temperature in Cy3-conjugated or Alexa 488-conjugated (Jackson Immunoresearch) secondary antibodies at dilution 1:200 in PBS and cover-slipped with DAKO fluorescent mounting medium (Dako S3023). Images were obtained by fluorescence microscopy (Nikon Eclipse TE300). For MAP2 and Synapsin 1 analysis, fluorescence images of 2048 × 2048 pixels (6.5 μm/pixel) were acquired with oil objective 60×/NA 1.42 (Olympus) on an Olympus iX73 microscope equipped with an X-Light V3 spinning disc head (CrestOptics), an LDI laser illuminator (89 North), a PRIME cMOS camera and a MetaMorph software (Molecular Devices). Stack images (z-step of 0.3 μm) were analyzed with the ImageJ software, flattened in a maximum intensity Z-projection of 13 slices. MAP2 staining was used to identify segments of 50 μm. Synapsin 1 puncta was counted within each segment. Results were exported in an Excel file and data was plotted in GraphPad Prism version 8.0 for Mac (GraphPad Software, San Diego, California, USA; www.graphpad.com). The analysis was performed on 10 MAP2-positive segments from two independent batches of cultures.

4.9 | Preparation of cell lysates

Lysates of HEK-293 cells were obtained using a lysis buffer (150 mM NaCl, 10 mM Tris pH 8.0, Nonidet P40 0.5%) supplemented with a protease inhibitor cocktail (Sigma-Aldrich). Lysis was performed for 15 min on ice, followed by centrifugation at 14 000*g* for 15 min at 4°C. Protein concentration was determined by the Bradford assay.

4.10 | Sodium dodecyl sulfate-polyacrylamide gel electrophoresis (SDS-PAGE) and western blot

Fifty μg of proteins or equal amounts of cell culture medium from NLGN3 (WT or R451C) expressing cells were subjected to SDS-PAGE

(10% v/v polyacrylamide gel) in running buffer (25 mM Tris pH 8.3, 0.19 M glycine, 0.1% sodium dodecyl sulfate) and transferred to polyvinylidene difluoride membrane (Merck-Millipore) in transfer buffer (25 mM Tris pH 8.3, 0.19 M glycine). The membrane was blocked with 5% (w/v) nonfat dried milk powder in tween-tris-buffered saline (T-TBS) (Low Fat Dry Milk) or with 1% (w/v) bovine serum albumin (BSA) in PBS (2.68 mM KCl, 1.47 mM KH_2PO_4, 0.137 M NaCl, 10.16 mM Na_2HPO_4). Primary antibodies were diluted in PBS added with 1% BSA and 0.1% sodium azide at the following dilution: anti-FLAG M2 1:1000 (mouse, Sigma-Aldrich no. F3165), anti-GR 1:1000 (rabbit, Cell Signaling Technology), anti-P-GR 1:1000 (rabbit, Cell Signaling Technology), anti-ATF6 1:1000 (mouse, Bio Academia), anti-KDEL (detecting ER-resident proteins including BiP and GRP94) 1:1000 (mouse, Enzo Life Sciences), anti-PDI 1:1000 (rabbit, Enzo Life Sciences), anti-total eIF2alpha 1:1000 (mouse, no. L57A5 Cell Signaling), anti-P-eIF2apha (Ser51) 1:1000 (rabbit, no. 119A11 Cell Signaling), anti-GRP78 BiP antibody (1:1000, rabbit, Abcam no. ab21685), anti-Actin 1:1000 (mouse, Millipore no. MAB1501), anti-NLGN1 (1:1000, mouse, Synaptic Systems), anti-NLGN2 (1:1000, rabbit, Synaptic Systems), anti-NLGN3 (1:1000, rabbit, Synaptic Systems), and antigen-purified rabbit polyclonal anti-NS (1 μg/mL).[31]

Horseradish peroxidase (HRP) conjugated secondary antibodies, goat–antimouse and goat–antirabbit (Sigma-Aldrich, Milan, Italy) were diluted 1:10000 in 5% (w/v) nonfat dried milk powder in T-TBS. All the incubations were performed for 1 h at room temperature. The HRP signal has been detected by using ECL (HyGLO, Denville Scientific Inc.), visualized and recorded by a ChemiDoc system (BioRad).

4.11 | Immunostaining of HEK-293 cells

HEK-293 cells (100 000 cells/well) were plated on glass coverslips coated with 0.5 mg/mL poly-D-lysine (Sigma-Aldrich) in 24-well plates and treated with selected compounds for 48 h. Untreated cells cultured in the same conditions were used as control. Cells were washed with ice-cold PBS and fixed with 4% paraformaldehyde (PFA, Sigma-Aldrich) for 20 min at room temperature, followed by fixation with prechilled methanol (Sigma-Aldrich) for 15 min at −20°C. The blocking step was performed for 1 h at room temperature using a solution containing 2% normal sheep serum, 0.1% Triton-X 100, 0.02% sodium azide in PBS. The same solution has been used for diluting primary and secondary antibodies. Anti-FLAG (1:5000, Rabbit, Sigma-Aldrich no. F7425) and anti-calreticulin (1:500, Mouse, Enzo ADI-SPA601) were incubated in combination, overnight at 4°C, while fluorescent secondary antibodies Cy3-anti-rabbit (donkey, Jackson Immuno Research no. 711–165-152) and Alexa Fluor 488-anti-mouse (donkey, Jackson Immuno Research no. 715–545-151) were diluted 1:500 and incubated 1 h at room temperature. Nuclei were stained with 4',6-diamidino-2-phenylindole, dihydrochloride (DAPI) (Calbiochem) 1:1000 in PBS for 10 min. Fluorescent signal was detected by confocal microscope (Zeiss) at 63× magnification and colocalization analysis was obtained on Z-stack images using the JACoP plugin of the NIH software ImageJ as previously described.[63] Mander's overlap coefficient M1 was calculated for at least 15 cells/experiment. For the analysis of UPR reporter plasmid, HEK-293 cells (100 000 cells/well) were plated on glass coverslips coated with 0.5 mg/mL poly-D-lysine (Sigma-Aldrich) in 24-well plates and transfected with the fluorescent reporter plasmids XBP1[36] using PEI (Sigma-Aldrich). After 3 h, cells were treated with DEX for an additional 48 h. Untreated cells cultured in the same conditions were used as control. Cells were washed with ice-cold PBS and fixed with 4% PFA (Sigma-Aldrich) for 20 min at room temperature. Nuclei were stained with DAPI (Calbiochem). Cells were counted using a fluorescence microscope (Zeiss Axioskop2) with a 40× objective. Five fields were randomly selected for each slide, and green fluorescent cells were counted in each field. The number of green fluorescent cells was then divided by the number of total cells revealed by the DAPI and then normalized to untreated condition. Statistical analysis was carried out on the ratio of green fluorescent cells/total cells for each field.

4.12 | FACS analysis

Approximately 800 000 cells/well were plated in six-well plates. After seeding, cells were treated with selected compounds for 48 h. Untreated cells cultured in the same conditions were used as control. PBS added with 1 mM EDTA and 2% FBS was used for harvesting cells, as well as for the washing steps and for diluting the antibodies. Surface-localized NLGN3 was stained with anti-FLAG M2 (1:1000, mouse Sigma) for 1 h on ice. After two washes, FITC-conjugated rat antimouse (1:20) IgG1 secondary antibody was incubated for 20 min at 4°C. The fluorescence signal was detected with a BD FACS Canto II Becton Dickinson (San Jose, California, USA) and flow cytometry profiles were analyzed using FACS Diva Software version 6.0. Dead cells were excluded from the analysis by Forward/Side scatter gating. A minimum of 10 000 gated events on living cells were collected per data set.

4.13 | Cocultures of HEK-293 cells and hippocampal neurons

Primary hippocampal neuronal cultures were prepared from 0 to 2-postnatal day-old (P0–P2) C57BL/6 mice. Briefly, after dissection from diencephalic structures, the meninges were removed, and hippocampal tissues chopped and digested for 30 min at room temperature in 30 U papain (Worthington Biochemical Corporation) and Hank's balanced salt solution (HBSS, Gibco™). Cells were washed twice with HBSS to remove the excess of papain, and mechanically dissociated in basal medium Eagle (Gibco™) supplemented with 10% FBS (Gibco™), 0.45% glucose (Sigma Aldrich), 100 mM sodium pyruvate (Sigma Aldrich), 100 mM Hepes buffer, and Mito+ serum extender (1:1000, Sigma Aldrich). Cells were plated at a density of 10×10^3 in the same medium on 100 mg/mL poly-L-lysine-coated 12 mm cover glasses (Gibco™). After 2 h, the medium was replaced with serum-free Neurobasal/B27 (Gibco™) and cells were kept at 37°C in 5% CO_2. Two days later, 5 μM cytosine a-D-arabinofuranoside hydrochloride (AraC, Sigma Aldrich) was added to the medium. On day 7 in vitro, WT or R451C NLGN3 expressing HEK-293 cells were seeded at a density of 50×10^3 on the

hippocampal neurons in the same medium. One day later, mixed cultures were treated with 2 μM DEX for an additional 48 h.

4.14 | Cocultures immunostaining and image analysis

Cocultures of HEK-293 cells (WT and R451C NLGN3) and hippocampal neurons attached onto PLO/Laminin-coated round cover glasses were fixed with 4% PFA (Sigma Aldrich) for 15 min at room temperature, washed three times with PBS (Thermo Fisher Scientific), permeabilized with PBS containing 0.2% Triton X-100 (Sigma Aldrich) for 15 min and then blocked for 45 min at room temperature with a PBS solution containing 0.1% Tween-20 (Sigma Aldrich) and 5% goat serum (Merck). The following primary antibodies were prepared in blocking buffer and incubated overnight at 4°C: anti-FLAG (rabbit, 1:500, Sigma Aldrich no. F7425), anti-MAP2 (chicken, 1:200, Abcam ab5392), anti-VGLUT1 (mouse, 1:250, Sigma Aldrich SAB5200258). On the next day, the primary antibodies solution was tipped off, and the cells washed three times with a PBS solution containing 0.1% Tween-20. The secondary antibodies Goat antichicken Alexa Fluor™ 594, Goat antimouse Alexa Fluor™ 488 and Goat antirabbit Alexa Fluor™ 647 (1:750, all from ThermoFisher Scientific) were prepared in blocking buffer and incubated for 1 h at room temperature. Cells were then washed three times with a PBS solution containing 0.1% Tween-20. In order to prepare the cells for analysis, round cover glasses with attached and stained cells were sealed with rectangular ones using the PROLONG liquid mountant with DAPI to stain nuclei (ProLong™ Diamond Antifade Mountant with DAPI, P36962, Invitrogen). The specificity of the staining was tested by performing control experiments in the absence of primary antibody incubation. For fluorescent image analysis, three independent batches of cultures for each condition were carried out. Fluorescence images of 2048 × 2048 pixels (6.5 μm/pixel) were acquired with oil objective 60×/NA 1.42 (Olympus) on an Olympus iX73 microscope equipped with an X-Light V3 spinning disc head (CrestOptics), an LDI laser illuminator (89 North), a PRIME cMOS camera and a MetaMorph software (Molecular Devices). Stack images (z-step of 0.3 μm) were analyzed with the ImageJ software, flattened in a maximum intensity Z-projection of 13 slices. For each channel, stacked images were adjusted in the grayscale using an automatic thresholding method (IsoData algorithm-Default) to subtract the background noise. Subsequently, in the FLAG channel a mask was created and transferred to the VGLUT1 channel. The synaptic quantification within the mask was analyzed measuring the % of the FLAG area covered by VGLUT1 signal. At the end of the analysis results were exported in an Excel file and data were plotted in GraphPad Prism version 8.0 for Mac (GraphPad Software, San Diego, California, USA; www.graphpad.com). The analysis was performed on 15 images per condition. Primary hippocampal neuronal cultures were treated with DEX and analyzed as a control group to validate the results. The synaptic quantification was performed counting the number of VGLUT1 puncta (15 fields per condition).

4.15 | Real time-RT-PCR

Total RNA was extracted from WT or R451C NLGN3 NSPCs expressing cells by using Trizma (SIGMA) and following the manufacturer's procedures. The total RNA concentration and purity were examined by the ratio A260/280 values obtained by Nanodrop (Thermo Fisher) and DNase I turbo treatment (Ambion, Thermo Fisher Scientific, Milan, Italy) was used to avoid genomic DNA contamination. First-strand cDNA was synthesized using SensiFAST™ cDNA (Bioline) starting from 1 μg of RNA according to the manufacturer's specifications. cDNA was subjected to real-time RT-PCR by using SYBR™ Green 2× (Applied BiosystemsTM) and amplified for 40 cycles with 15 s at 95°C followed by 60 s at 60°C. Real-time RT-PCR was carried out using a thermocycler QuantStudio™ 3 System (Thermo Fisher). All assays were run in triplicate and relative quantification was carried out using the comparative CT method.

Used primer sets were: β-Actin FW (5′-3′)-TGACAGGATGC AGAAGGAGA and REV (5′-3′)-GTACTTGCGCTCAGGAGGAC; NLGN3 FW (5′-3′)-TACTTCTACGCCTTCTACCAT and REV (5′-3′)-GCAAAGTTGGTCCAATAGGT.

4.16 | Calcium signal measurements

NSPCs were differentiated into neuronal, either WT or R451C, cultures for 15 days onto eight-well chambers previously coated with poly-ornithine/laminin. For Fluo-4 studies, neuronal cultures were subjected to 5 μM Fluo-4 AM, which was excited with a 488 nm (Thermo Fisher) in a serum-free culture medium for 45 min at 37°C. The time baseline (NES [normal KCl]: NaCl 140, KCl 2.8, $MgCl_2$ 2, $CaCl_2$ 2, Glucose 10, HEPES 10 mM) lapse series were taken at intervals of every 500 ms for a period of 1 min to capture the Ca^{2+} oscillations. After monitoring baseline oscillations, neurons were depolarized for 10 s by adding NES (high KCl) NaCl 90, KCl 52.8, $MgCl_2$ 2, $CaCl_2$ 2, Glucose 10, HEPES 10 mM. Data are presented as the relative change in fluorescence ($\Delta F/F0$), where $F0$ is basal fluorescence and $\Delta F = F - F0$. Responses to KCl-stimuli were analyzed as fluorescence change, expressed as $\Delta F/F0$ (fluorescence change normalized on baseline). An average graph has been created to show average responses in WT and R451C cultures. The range of responses was calculated for each cell using the Clampfit software. From the average graph, T1/2 was calculated, that is the time between the peak and the point where the peak is halfway through its total amplitude.

4.17 | Statistical analysis

All experiments were performed at least three times on independent biological samples, as indicated in the figure legends. Student's *t*-test was used for statistical analysis by using Prism8 (GraphPad Prism version 8.0 for Mac): $^{*}p < 0.05$, $^{**}p < 0.01$, $^{***}p < 0.001$, $^{****}p < 0.0001$.

AUTHOR CONTRIBUTIONS

ADJ, DC, EC, TD, LT, SDA, AS, and EM contributed to the study conception and design. Material preparation, data collection, and analysis were performed by TD, LT, RG, FS, LM, LF, CL, SB, CP, SG, RS, EG, AS, DR, EM, SDA, EC, and ADJ. The first draft of the article was written by TD and ADJ, and all authors commented on previous versions of the article. TD prepared the graphical abstract. All authors read and approved the final version of the article.

ACKNOWLEDGMENTS

This research was partially funded by the REGIONE LAZIO (19036AP000000019 and A0112E0073 to SDA); Fulbright Award (FSP-P005556 to SDA). This research was partially funded by grants from Sapienza University (to SDA) and by the D-Tails-IIT JointLab (to SDA). LM was also supported by the PhD program in Life Science at Sapienza University of Rome. This study was supported by grants from the Robert Wood Johnson Foundation to the Child Health Institute of New Jersey (RWJF grant no. 74260), the Governor's Council for Medical Research and Treatment of Autism (CAUT16APL020 to DC).

CONFLICT OF INTEREST STATEMENT

Silvia Di Angelantonio is a member of the scientific advisory board of D-Tails s.r.l. The remaining authors declare that the research was conducted in the absence of any commercial or financial relationships that could be construed as a potential conflicts of interest.

PEER REVIEW

The peer review history for this article is available at https://www.webofscience.com/api/gateway/wos/peer-review/10.1111/tra.12930.

DATA AVAILABILITY STATEMENT

All the data generated in this study is reported in the figures, tables, and supplementary figures that are part of this article.

ORCID

Lorenza Mautone https://orcid.org/0000-0002-0510-1420
Raimondo Sollazzo https://orcid.org/0000-0002-6594-231X
Antonella De Jaco https://orcid.org/0000-0002-9394-0207

REFERENCES

1. Liu X, Hua F, Yang D, et al. Roles of neuroligins in central nervous system development: focus on glial neuroligins and neuron neuroligins. *J Transl Med*. 2022;20(1):418. doi:10.1186/s12967-022-03625-y
2. de la Torre-Ubieta L, Won H, Stein JL, Geschwind DH. Advancing the understanding of autism disease mechanisms through genetics. *Nat Med*. 2016;22(4):345-361. doi:10.1038/nm.4071
3. Baig DN, Yanagawa T, Tabuchi K. Distortion of the normal function of synaptic cell adhesion molecules by genetic variants as a risk for autism spectrum disorders. *Brain Res Bull*. 2017;129:82-90. doi:10.1016/j.brainresbull.2016.10.006
4. Trobiani L, Meringolo M, Diamanti T, et al. The neuroligins and the synaptic pathway in autism spectrum disorder. *Neurosci Biobehav Rev*. 2020;119:37-51. doi:10.1016/j.neubiorev.2020.09.017
5. Bemben MA, Nguyen Q-A, Wang T, Li Y, Nicoll RA, Roche KW. Autism-associated mutation inhibits protein kinase C-mediated neuroligin-4X enhancement of excitatory synapses. *Proc Natl Acad Sci USA*. 2015;112(8):2551-2556. doi:10.1073/pnas.1500501112
6. Jeong J, Paskus JD, Roche KW. Posttranslational modifications of neuroligins regulate neuronal and glial signaling. *Curr Opin Neurobiol*. 2017;45:130-138. doi:10.1016/j.conb.2017.05.017
7. Südhof TC. Synaptic neurexin complexes: a molecular code for the logic of neural circuits. *Cell*. 2017;171(4):745-769. doi:10.1016/j.cell.2017.10.024
8. Südhof TC. Towards an understanding of synapse formation. *Neuron*. 2018;100(2):276-293. doi:10.1016/j.neuron.2018.09.040
9. Jamain S, Quach H, Betancur C, et al. Mutations of the X-linked genes encoding neuroligins NLGN3 and NLGN4 are associated with autism. *Nat Genet*. 2003;34(1):27-29. doi:10.1038/ng1136
10. Talebizadeh Z, Lam DY, Theodoro MF, Bittel DC, Lushington GH, Butler MG. Novel splice isoforms for NLGN3 and NLGN4 with possible implications in autism. *J Med Genet*. 2006;43(5):e21. doi:10.1136/jmg.2005.036897
11. Yan J, Oliveira G, Coutinho A, et al. Analysis of the neuroligin 3 and 4 genes in autism and other neuropsychiatric patients. *Mol Psychiatry*. 2005;10(4):329-332. doi:10.1038/sj.mp.4001629
12. Nakanishi M, Nomura J, Ji X, et al. Functional significance of rare neuroligin 1 variants found in autism. *PLoS Genet*. 2017;13(8):e1006940. doi:10.1371/journal.pgen.1006940
13. Nguyen TA, Lehr AW, Roche KW. Neuroligins and neurodevelopmental disorders: X-linked genetics. *Front Synaptic Neurosci*. 2020;12:33. doi:10.3389/fnsyn.2020.00033
14. Ribeiro LF, Verpoort B, de Wit J. Trafficking mechanisms of synaptogenic cell adhesion molecules. *Mol Cell Neurosci*. 2018;91:34-47. doi:10.1016/j.mcn.2018.04.003
15. De Jaco A, Comoletti D, Kovarik Z, et al. A mutation linked with autism reveals a common mechanism of endoplasmic reticulum retention for the alpha,beta-hydrolase fold protein family. *J Biol Chem*. 2006;281(14):9667-9676. doi:10.1074/jbc.M510262200
16. De Jaco A, Lin MZ, Dubi N, et al. Neuroligin trafficking deficiencies arising from mutations in the alpha/beta-hydrolase fold protein family. *J Biol Chem*. 2010;285(37):28674-28682. doi:10.1074/jbc.M110.139519
17. Comoletti D, De Jaco A, Jennings LL, et al. The Arg451Cys-neuroligin-3 mutation associated with autism reveals a defect in protein processing. *J Neurosci*. 2004;24(20):4889-4893. doi:10.1523/JNEUROSCI.0468-04.2004
18. Chih B, Afridi SK, Clark L, Scheiffele P. Disorder-associated mutations lead to functional inactivation of neuroligins. *Hum Mol Genet*. 2004;13(14):1471-1477. doi:10.1093/hmg/ddh158
19. Tabuchi K, Blundell J, Etherton MR, et al. A neuroligin-3 mutation implicated in autism increases inhibitory synaptic transmission in mice. *Science*. 2007;318(5847):71-76. doi:10.1126/science.1146221
20. Gioia R, Seri T, Diamanti T, et al. Adult hippocampal neurogenesis and social behavioural deficits in the R451C Neuroligin3 mouse model of autism are reverted by the antidepressant fluoxetine. *J Neurochem*. 2022;165:318-333. doi:10.1111/jnc.15753
21. Trobiani L, Favaloro FL, Di Castro MA, et al. UPR activation specifically modulates glutamate neurotransmission in the cerebellum of a mouse model of autism. *Neurobiol Dis*. 2018;120:139-150. doi:10.1016/j.nbd.2018.08.026
22. Hetz C, Zhang K, Kaufman RJ. Mechanisms, regulation and functions of the unfolded protein response. *Nat Rev Mol Cell Biol*. 2020;21(8):421-438. doi:10.1038/s41580-020-0250-z
23. Ulbrich L, Favaloro FL, Trobiani L, et al. Autism-associated R451C mutation in neuroligin3 leads to activation of the unfolded protein response in a PC12 Tet-on inducible system. *Biochem J*. 2016;473(4):423-434. doi:10.1042/BJ20150274

24. Quartier A, Courraud J, Thi Ha T, et al. Novel mutations in NLGN3 causing autism spectrum disorder and cognitive impairment. *Hum Mutat*. 2019;40(11):2021-2032. doi:10.1002/humu.23836
25. Chadwick SR, Lajoie P. Endoplasmic reticulum stress coping mechanisms and lifespan regulation in health and diseases. *Front Cell Dev Biol*. 2019;7:84. doi:10.3389/fcell.2019.00084
26. Marciniak SJ, Chambers JE, Ron D. Pharmacological targeting of endoplasmic reticulum stress in disease. *Nat Rev Drug Discov*. 2022;21(2):115-140. doi:10.1038/s41573-021-00320-3
27. Goffredo D, Conti L, Di Febo F, et al. Setting the conditions for efficient, robust and reproducible generation of functionally active neurons from adult subventricular zone-derived neural stem cells. *Cell Death Differ*. 2008;15(12):1847-1856. doi:10.1038/cdd.2008.118
28. Azoulay-Ginsburg S, Trobiani L, Setini A, et al. A lipophilic 4-phenylbutyric acid derivative that prevents aggregation and retention of misfolded proteins. *Chem Eur J*. 2020;26(8):1834-1845. doi:10.1002/chem.201904292
29. De Jaco A, Dubi N, Comoletti D, Taylor P. Folding anomalies of neuroligin3 caused by a mutation in the alpha/beta-hydrolase fold domain. *Chem Biol Interact*. 2010;187(1-3):56-58. doi:10.1016/j.cbi.2010.03.012
30. Van Moortel L, Thommis J, Maertens B, et al. Novel assays monitoring direct glucocorticoid receptor protein activity exhibit high predictive power for ligand activity on endogenous gene targets. *BioRxiv* March 30 2022. doi:10.1101/2022.03.29.486227
31. Guadagno NA, Moriconi C, Licursi V, et al. Neuroserpin polymers cause oxidative stress in a neuronal model of the dementia FENIB. *Neurobiol Dis*. 2017;103:32-44. doi:10.1016/j.nbd.2017.03.010
32. Davies MJ, Miranda E, Roussel BD, Kaufman RJ, Marciniak SJ, Lomas DA. Neuroserpin polymers activate NF-kappaB by a calcium signaling pathway that is independent of the unfolded protein response. *J Biol Chem*. 2009;284(27):18202-18209. doi:10.1074/jbc.M109.010744
33. Das I, Png CW, Oancea I, et al. Glucocorticoids alleviate intestinal ER stress by enhancing protein folding and degradation of misfolded proteins. *J Exp Med*. 2013;210(6):1201-1216. doi:10.1084/jem.20121268
34. Fujii Y, Khoshnoodi J, Takenaka H, et al. The effect of dexamethasone on defective nephrin transport caused by ER stress: a potential mechanism for the therapeutic action of glucocorticoids in the acquired glomerular diseases. *Kidney Int*. 2006;69(8):1350-1359. doi:10.1038/sj.ki.5000317
35. Namba T, Ishihara T, Tanaka K, Hoshino T, Mizushima T. Transcriptional activation of ATF6 by endoplasmic reticulum stressors. *Biochem Biophys Res Commun*. 2007;355(2):543-548. doi:10.1016/j.bbrc.2007.02.004
36. Iwawaki T, Akai R, Kohno K, Miura M. A transgenic mouse model for monitoring endoplasmic reticulum stress. *Nat Med*. 2004;10(1):98-102. doi:10.1038/nm970
37. Tanjore H, Lawson WE, Blackwell TS. Endoplasmic reticulum stress as a pro-fibrotic stimulus. *Biochim Biophys Acta*. 2013;1832(7):940-947. doi:10.1016/j.bbadis.2012.11.011
38. Walker TL, Kempermann G. One mouse, two cultures: isolation and culture of adult neural stem cells from the two neurogenic zones of individual mice. *J Vis Exp*. 2014;84:e51225. doi:10.3791/51225
39. Cacci E, Ajmone-Cat MA, Anelli T, Biagioni S, Minghetti L. In vitro neuronal and glial differentiation from embryonic or adult neural precursor cells are differently affected by chronic or acute activation of microglia. *Glia*. 2008;56(4):412-425. doi:10.1002/glia.20616
40. Soldati C, Caramanica P, Burney MJ, et al. RE1 silencing transcription factor/neuron-restrictive silencing factor regulates expansion of adult mouse subventricular zone-derived neural stem/progenitor cells in vitro. *J Neurosci Res*. 2015;93(8):1203-1214. doi:10.1002/jnr.23572
41. Etherton MR, Tabuchi K, Sharma M, Ko J, Südhof TC. An autism-associated point mutation in the neuroligin cytoplasmic tail selectively impairs AMPA receptor-mediated synaptic transmission in hippocampus. *EMBO J*. 2011;30(14):2908-2919. doi:10.1038/emboj.2011.182
42. Lock JT, Parker I, Smith IF. A comparison of fluorescent Ca^{2+} indicators for imaging local Ca^{2+} signals in cultured cells. *Cell Calcium*. 2015;58(6):638-648. doi:10.1016/j.ceca.2015.10.003
43. Yi F, Danko T, Botelho SC, et al. Autism-associated SHANK3 haploinsufficiency causes Ih channelopathy in human neurons. *Science*. 2016;352(6286):aaf2669. doi:10.1126/science.aaf2669
44. Perlini LE, Botti F, Fornasiero EF, et al. Effects of phosphorylation and neuronal activity on the control of synapse formation by synapsin I. *J Cell Sci*. 2011;124(Pt 21):3643-3653. doi:10.1242/jcs.086223
45. Xu X, Hu Z, Zhang L, et al. Not all neuroligin 3 and 4X missense variants lead to significant functional inactivation. *Brain Behav*. 2017;7(9):e00793. doi:10.1002/brb3.793
46. Chubykin AA, Liu X, Comoletti D, Tsigelny I, Taylor P, Südhof TC. Dissection of synapse induction by neuroligins: effect of a neuroligin mutation associated with autism. *J Biol Chem*. 2005;280(23):22365-22374. doi:10.1074/jbc.M410723200
47. De Jaco A, Comoletti D, King CC, Taylor P. Trafficking of cholinesterases and neuroligins mutant proteins. An association with autism. *Chem Biol Interact*. 2008;175(1–3):349-351. doi:10.1016/j.cbi.2008.04.023
48. Venkatesh HS, Johung TB, Caretti V, et al. Neuronal activity promotes glioma growth through Neuroligin-3 secretion. *Cell*. 2015;161(4):803-816. doi:10.1016/j.cell.2015.04.012
49. Venkatesh HS, Tam LT, Woo PJ, et al. Targeting neuronal activity-regulated neuroligin-3 dependency in high-grade glioma. *Nature*. 2017;549(7673):533-537. doi:10.1038/nature24014
50. Caohuy H, Jozwik C, Pollard HB. Rescue of DeltaF508-CFTR by the SGK1/Nedd4-2 signaling pathway. *J Biol Chem*. 2009;284(37):25241-25253. doi:10.1074/jbc.M109.035345
51. Chen M, Cai H, Klein JD, Laur O, Chen G. Dexamethasone increases aquaporin-2 protein expression in ex vivo inner medullary collecting duct suspensions. *Front Physiol*. 2015;6:310. doi:10.3389/fphys.2015.00310
52. Diamanti T, Prete R, Battista N, Corsetti A, De Jaco A. Exposure to antibiotics and neurodevelopmental disorders: could probiotics modulate the gut-brain Axis? *Antibiotics (Basel)*. 2022;11(12):1767. doi:10.3390/antibiotics11121767
53. Liu Z, Fei B, Xie L, et al. Glucocorticoids protect HEI-OC1 cells from tunicamycin-induced cell damage via inhibiting endoplasmic reticulum stress. *Open Life Sci*. 2021;16(1):695-702. doi:10.1515/biol-2021-0057
54. Mihailidou C, Panagiotou C, Kiaris H, Kassi E, Moutsatsou P. Crosstalk between C/EBP homologous protein (CHOP) and glucocorticoid receptor in lung cancer. *Mol Cell Endocrinol*. 2016;436:211-223. doi:10.1016/j.mce.2016.08.001
55. Woodward AM, Di Zazzo A, Bonini S, Argüeso P. Endoplasmic reticulum stress promotes inflammation-mediated proteolytic activity at the ocular surface. *Sci Rep*. 2020;10(1):2216. doi:10.1038/s41598-020-59237-3
56. Jia H, Yu Z, Ge X, Chen Z, Huang X, Wei Y. Glucocorticoid-induced leucine zipper protects noise-induced apoptosis in cochlear cells by inhibiting endoplasmic reticulum stress in rats. *Med Mol Morphol*. 2020;53(2):73-81. doi:10.1007/s00795-019-00232-7
57. Shang Y, Wang F, Bai C, et al. Dexamethasone protects airway epithelial cell line NCI-H292 against lipopolysaccharide induced endoplasmic reticulum stress and apoptosis. *Chin Med J*. 2011;124(1):38-44.
58. Fu J, Gao J, Liang Z, Yang D. PDI-regulated disulfide bond formation in protein folding and biomolecular assembly. *Molecules*. 2020;26(1):171. doi:10.3390/molecules26010171

59. Sacco R, Cacci E, Novarino G. Neural stem cells in neuropsychiatric disorders. *Curr Opin Neurobiol*. 2018;48:131-138. doi:10.1016/j.conb.2017.12.005
60. Klocke B, Krone K, Tornes J, Moore C, Ott H, Pitychoutis PM. Insights into the role of intracellular calcium signaling in the neurobiology of neurodevelopmental disorders. *Front Neurosci*. 2023;17:1093099. doi:10.3389/fnins.2023.1093099
61. Lupo G, Gioia R, Nisi PS, Biagioni S, Cacci E. Molecular mechanisms of neurogenic aging in the adult mouse subventricular zone. *J Exp Neurosci*. 2019;13:1179069519829040. doi:10.1177/1179069519829040
62. Sinno M, Biagioni S, Ajmone-Cat MA, et al. The matrix metalloproteinase inhibitor marimastat promotes neural progenitor cell differentiation into neurons by gelatinase-independent TIMP-2-dependent mechanisms. *Stem Cells Dev*. 2013;22(3):345-358. doi:10.1089/scd.2012.0299
63. Bolte S, Cordelières FP. A guided tour into subcellular colocalization analysis in light microscopy. *J Microsc*. 2006;224(Pt 3):213-232. doi:10.1111/j.1365-2818.2006.01706.x

SUPPORTING INFORMATION

Additional supporting information can be found online in the Supporting Information section at the end of this article.

How to cite this article: Diamanti T, Trobiani L, Mautone L, et al. Glucocorticoids rescue cell surface trafficking of R451C Neuroligin3 and enhance synapse formation. *Traffic*. 2024;25(1):e12930. doi:10.1111/tra.12930